Tetrahedron Green Chem 2 (2023) 100020

Contents lists available at ScienceDirect

Tetrahedron Green Chem

journal homepage: www.journals.elsevier.com/tetrahedron-green-chem

Formic acid as renewable reagent and product in biomass upgrading

Mahdi Achour [a,b], Débora Álvarez-Hernández [a], Estela Ruiz-López [a], Cristina Megías-Sayago [c], Fatima Ammari [b], Svetlana Ivanova [a,*], Miguel Ángel Centeno [a]

[a] Departamento de Química Inorgánica e Instituto de Ciencia de Materiales de Sevilla, Centro mixto CSIC-Universidad de Sevilla, 41092, Sevilla, Spain
[b] Laboratoire de Génie des Procédés Chimiques- LGPC, Département de Génie des Procéés, Faculté de Technologie, Université Ferhat Abbas Setif-1, 19000, Setif, Algeria
[c] Departamento de Química Inorgánica, Instituto de Investigaciones Químicas and Centro de Innovación en Química Avanzada (ORFEO-CINQA), Centro mixto CSIC-Universidad de Sevilla, 41092, Sevilla, Spain

ARTICLE INFO

Keywords:
Biomass upgrading
Formic acid
H-donor
Catalytic transfer reaction (CTH)
Hydrodeoxygenation (HDO) reaction
Levulinic acid

ABSTRACT

The problems associated with the use of molecular hydrogen (transportation, storage and high cost) have pushed scientists to the pursuit of efficient hydrogen donors, able to reduce chemical bonds in the presence of catalysts through catalytic transfer hydrogenation (CTH) reactions. In this sense, formic acid stands up as one of the most important and safest chemical molecules for H_2 generation under mild conditions. It can be obtained from biomass through different catalytic transformations and used as well to upgrade biomass to platform chemicals. This review summarizes the recently published studies dealing with formic acid production from biomass (using glucose as representing molecule) along with its use in hydrogen involved reactions of different groups of platform chemicals upgrading.

1. Introduction

The global energy demand associated with the continuous population growth starts alarming society on the unsustainable use of nonrenewable energy sources such as natural gas, coal, and crude oil [1]. In the last years, the risk of supply interruption has become even more important referring to the geopolitical conflicts and restriction policies. What is more, the uncontrolled energy consumption causes constant environmental pollution problems, that appeal to limit the fossil sources utilization in favor to a new, clean and sustainable sources for fuels and chemicals production [2,3].

In the last decades, biomass has become the most abundant, versatile and renewable source for fine chemicals and biofuels production in the world. Much efforts have been made to develop new technologies for biomass upgrading into high value-added chemicals [4]. The principal low-cost and sustainable biomass that can be used as feedstock is the lignocellulosic (LCB) one with its three main components: cellulose, hemicellulose and lignin. These macromolecules could originate after hydrolysis a *fan* of platform molecules, useful to synthesize a wide spectrum of valuable chemicals (sugars, acids and aromatics) [5,6]. The key processes to transform these molecules into chemicals and biofuels are hydrogenation and hydrogenolysis reactions. The former increases the ratio of hydrogen to carbon by using hydrogen from some external sources and the latter cleaves carbon-carbon or carbon-heteroatom bonds in presence of H_2. In the particular case of biomass we often refer to hydrodeoxygenation (HDO) as a hydrogenolytic reaction in connection to the reduction of oxygen content of all LCB derived molecules [7,8]. The main challenge of the HDO mediated processes is to remove as much oxygen as possible while using the least possible amount of hydrogen [9]. Molecular hydrogen (H_2) has been frequently reported as hydrogen donor for HDO processes due to its beneficial activation potential on a wide range of metal surfaces and on its availability [8]. Nevertheless, its use presents some considerable issues owing to the high pressure H_2 over-utilization, and its high cost and safety hazards during transportation, storage, and use. It also presents a low solubility in most solvents, being required a high H_2 pressure to achieve satisfactory conversions and yields without the production of high amounts of by-products [10].

In this sense, some organic molecules have demonstrated to act as hydrogen donors for the reduction of chemical bonds in presence of catalysts through a catalytic transfer hydrogenation (CTH) reaction. Its use avoids the need for complicated installations and harsh conditions [11] being also environmentally friendly and economically viable [12,13]. Several hydrogen donors, such as alcohols, organic acids and

* Corresponding author.
E-mail addresses: mahdiachour02@gmail.com (M. Achour), debora.alvarez@icmse.csic.es (D. Álvarez-Hernández), eruizl@us.es (E. Ruiz-López), cmegias@us.es (C. Megías-Sayago), ammarifatima@yahoo.fr (F. Ammari), svetlana@icmse.csic.es, sivanova@us.es (S. Ivanova), centeno@icmse.csic.es (M.Á. Centeno).

https://doi.org/10.1016/j.tgchem.2023.100020
Received 30 March 2023; Received in revised form 11 July 2023; Accepted 12 July 2023
Available online 15 July 2023

hydrazine have been used in the CTH process [8,14] and, unlike molecular hydrogen, they may interact effectively in liquid phase thus enhancing the reactivity of the generated hydrogen [11]. Within the group of organic molecules, one of the most interesting hydrogen sources is formic acid (FA) [15,16], which quickly and selectively decomposes into H_2 and CO_2 under mild conditions [17–19]. FA has been recently identified as one of the most important and safest chemical molecules for H_2 storage, having a high volumetric hydrogen content, 26.5 M of H_2 (53 g H_2/L) reserved in 1 L of FA. For comparison, 1 L of gaseous H_2 is equivalent to 9.8 M and must be stored at a pressure of 22 MPa [17]. All these properties convert FA in an efficient hydrogen carrier with a high flash point (69 °C vs. 11 °C for methanol and −23 °C for gasoline), low inflammability [20], and biodegradability. Currently, FA is industrially produced using a fossil-based process, *i.e.,* carbonylation of methanol [21], although its large-scale production from biomass is also available [22]. Up to now, continuous attempts have been made to obtain FA from renewable sources through green routes, particularly starting with biomass or CO_2 [23,24], being the former feedstock summarized later in this review.

Hydrogen is generated from FA via dehydrogenation (Scheme 1) but, depending on the reaction conditions and the catalyst' nature, the dehydration reaction can also occur with release of CO. In general, this side reaction must be completely avoided not only because CO can be very poisonous for the catalysts [25], but also because its conversion to CO_2 and H_2 is conditioned by the water gas shift equilibrium [26].

A DFT study [27] resumes the FA decomposition into two pathways (Scheme 2):i) the carboxyl pathway (COOH), involving C–H bond splitting and followed by O–H break and ii) the formate pathway (HCOO), where the decomposition starts with O–H bond cleavage. In the case of the carboxyl route, the final products selectivity relies on the O–H or C–OH dissociations, leading to dehydrogenation and dehydration products in the first and second case, respectively. Regarding the formate pathway, it is possible to form a stable bidentate ($HCOO_B$) or monodentate ($HCOO_M$), resulting both in CO_2 and H_2 formation after C–H bond splitting. The strength of the metal(catalyst)-oxygen coordination would determine the decomposition pathway, being particularly important bidentate ($HCOO_B$) to monodentate ($HCOO_M$) complex transition in the final products distribution [27–29].

The employed catalysts have a major impact on the reactivity and selectivity of these routes [30]. In the last decade, various catalytic systems [31] have been reported for *in situ* hydrogen generation: i) homogeneous non-noble transition metal complexes based on cobalt [32], iron carbonyl [33], manganese [34], nickel [35,36] and copper [37,38]; ii) noble metal complexes based on ruthenium [39–41], iridium [42,43] or palladium [44] for which the control of activity and stability relied on a careful design of the ligand [45]; and iii) heterogeneous catalysts based on monometallic Pd [46–49], Au [50,51], Ru [52] and bimetallic PdAu [53], PdCo [54] formulations. At this point we must specify that a great variety of the catalysts mentioned above for *in situ* hydrogen production can also serve for CTH/HDO reactions and they are the object of this review. Without pretending to summarize all reported information, we have tried to regroup the recently published studies of formic acid production from biomass (using glucose as representing molecule) and its use in CTH/HDO reactions of various groups of platform chemicals.

2. Direct production of formic acid from biomass

Formic acid has multiple uses across industries (agricultural, food or chemical mainly) and its popularity has noticeably increased with the development of scaled-up methods for its production [55]. These methods can be grouped in three categories: methyl formate hydrolysis after methanol carbonylation; carbon dioxide hydrogenation and biomass treatment [56]. As a general drawback of the processes, we can mention i) the use of fossil resources, ii) the formation of undesirable products or iii) the use of harsh conditions. That is why, there is a renewed scientific interest for adopting sustainable and green chemistry practices able to reduce the environmental impact of the production processes [57–60]. Thus, all new technologies should include a renewable feedstock, reduce wastes and emissions, and develop more efficient and less toxic chemicals and processes. FA production from biomass meets all these criteria [61]. Glucose (GLC) is often used as a model molecule for LCB because of its prevailing concentration. Nevertheless, its oxidation selectivity is conditioned by the complexity of its molecule and the nature of the used catalysts. The selectivity to formic acid is often decreased by the presence of products of isomerization and retro-aldol reaction and different products of C–C cleavage (Scheme 3). Thus, the nature of oxidant and catalyst (acidity/basicity or redox behavior) plays a primordial role for achieving good selectivity during the process.

2.1. Hydrogen peroxide as the oxidant

Aluminum triflate ($Al(OTf)_3$) is a well-known Lewis acid catalyst, particularly active in reactions (oxidation included) that involve water as reactant and solvent [62]. Kong et al. [63] used that catalyst to convert glucose to formic acid in mild conditions (70 °C and reaction time of 12 h) using GLC to oxidant (H_2O_2), ratio of 1:10, and acetonitrile as additive. They achieved a high conversion rate of glucose (85%) but a very low FA yield (6.8%). The main product, glycolic acid, indicated that Lewis acid materials catalyzed glucose to fructose isomerization prior to its oxidation thus significantly decreasing the FA selectivity.

Takagaki and co-workers [64] found that alkaline metallic oxides possess a good catalytic activity in glucose oxidation to formic acid and related it to solid' basicity. CaO appears as the most active with 21% FA yield with fructose as a trace product. Reaction parameter optimization indicates glucose/H_2O_2 molar ratio of 1/5 in water, 90 °C temperature and 2 h time as optimal conditions to achieve full conversion and 45% FA yield. During the reaction the catalyst was gradually transformed into $CaCO_3$ diminishing the activity in the second cycle but recovering it after calcination at 800 °C. Wu et al. [65] investigated the use of MgO as catalyst and found high FA yield (78%) and conversion (90%) under mild conditions (50 °C, 4 h) with a stoichiometric GLC/H_2O_2 ratio. However, the catalyst also produced undesired products such as lactic

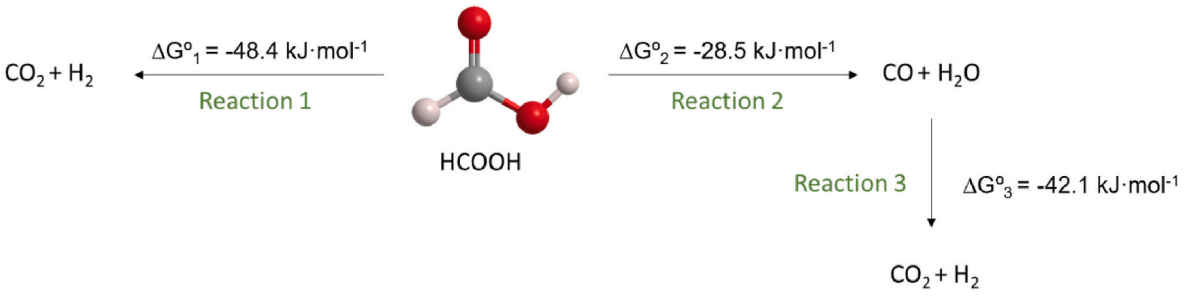

Scheme 1. Formic acid decomposition reaction in gas phase.

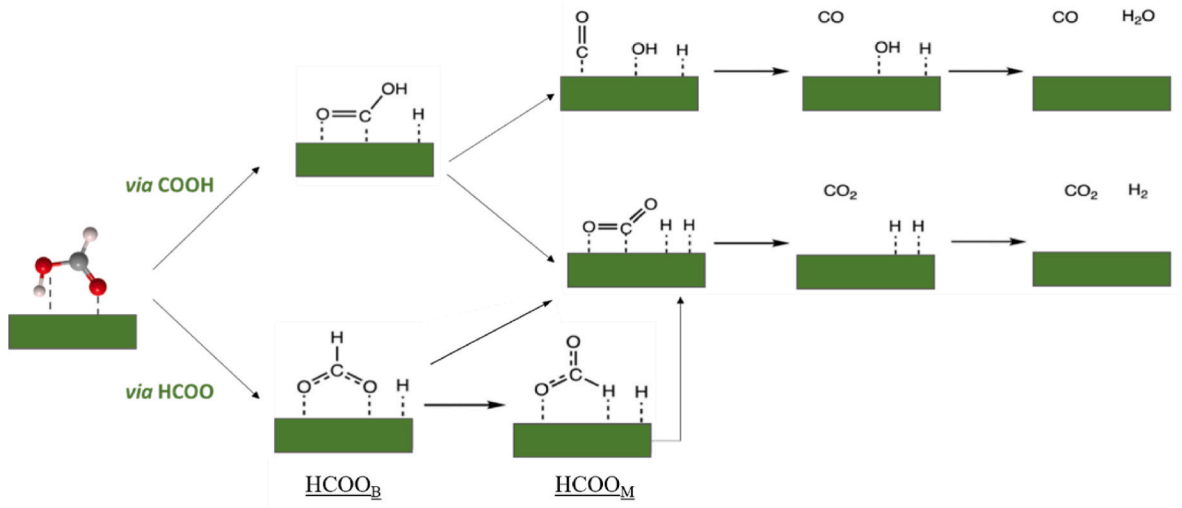

Scheme 2. Formic acid decomposition via carboxyl (top) and formate (bottom) intermediates, adapted from Ref. [27] with permission from the Royal Society of Chemistry.

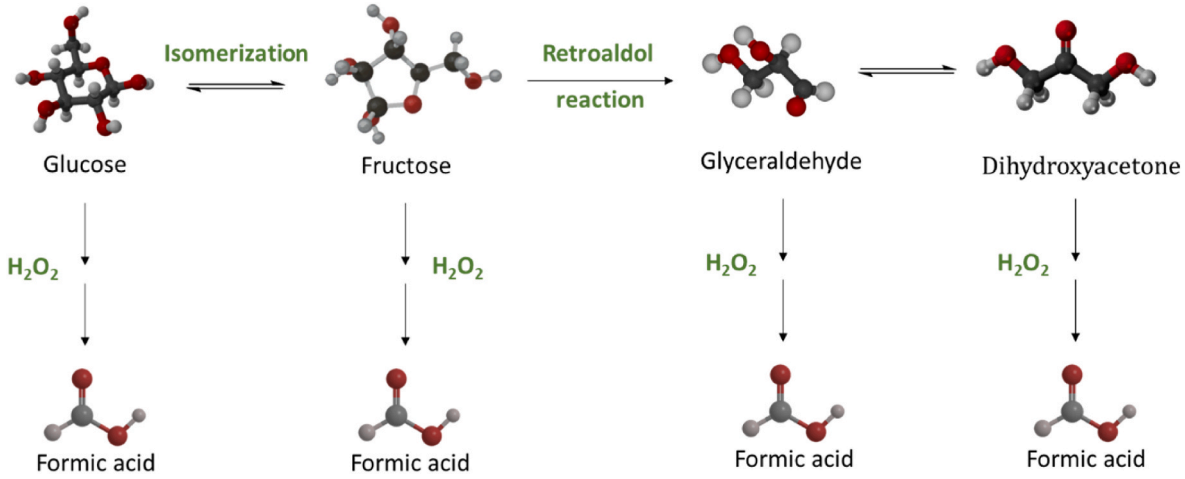

Scheme 3. Formic acid production from glucose and related reactions.

acid and arabinose. The catalytic activity of MgO catalyst was maintained through multiple cycles (up to 5) although a calcination between cycles was required.

Kılıç et al. [66] investigated the use of hydrotalcite-like materials as catalysts for the oxidation of GLC to FA in ethanol and evaluated the influence of Mg/Al ratio. No significant differences were found for the bare materials (hydrotalcites without calcination) but after treatment higher conversion was observed at higher Mg/Al ratios. The highest conversion (38.7%) with complete selectivity towards FA was achieved for Mg/Al ratio of 1/3. This study also reported a decrease in activity in the 4th catalytic cycle. In a recent publication, the same authors used bimetallic oxides as catalysts in similar conditions [67]. The highest conversion of 29% was achieved with Sr–Fe oxides calcined at 200 °C in comparison to the highest GLC conversion of 62% with FA yield of 10% reported for the Mg–Al oxides. The change of the solvent from ethanol to water decreases GLC conversion for the Mg–Al catalyst to 30% but increases the FA selectivity to 60%.

A novel silica-encapsulated heteropoly acid (HPAs) catalyst was studied by Yuan et al. [68] for the oxidation of several biomass platform molecules. Even though HPAs showed great redox properties, their low surface area and high solubility in polar solvents are considered as disadvantages for this reaction. That is why its encapsulation was proposed in this study and resulted in conversions close to 25% with increased FA selectivity (67%).

2.2. Molecular oxygen as the oxidizing agent

Albert [69] reported a series of heteropolyacids (HPA) with different vanadium/molybdenum ratios within the Keggin structure and found that the highest FA yield of 26% was given by the HPA-4 ($H_7PV_4Mo_8O_{40}$) sample at 90 °C and 20 bars of O_2 pressure after 8 h of reaction. The authors conclude that at least two vanadium atoms are needed within the polyoxometalate structure to produce some formic acid. Within the same group of catalysts, Reichert and Albert [70] compared HPA-5 ($H_8PV_5Mo_7O_{40}$) to HPA-2 ($H_5PV_2Mo_{10}O_{40}$) structures and found that the difference in activity arises from vanadium content, highest the content highest the glucose conversion. In this sense, higher vanadium content in HPA-5 results in more VO^{2+} liberation, presumably the active species. Nevertheless, the selectivity towards formic acid remains the same for both catalysts at around 68%.

Maerten et al. [71] also studied HPA-5 catalysts in water at 90 °C and 20 bars of O_2 and reported a 55% FA yield and 45% carbon dioxide (CO_2) yield. The change of the solvent to ethanol allowed a full yield towards methyl formate. The results of ^{13}C labelled glucose study confirmed that the formic acid unit is produced from this molecule and not from oxidation and esterification of the solvent. This study also

proposed a mechanism for glucose oxidation in ethanol that involves C–C cleavage producing erythrose on first step and glyoxal and glycolaldehyde after additional C–C breaking. These 2-carbon intermediates are then oxidized to formic acid forming rapidly methyl formate through esterification (Scheme 4). The study did not observe any other intermediates or CO_2.

Albert et al. [73] continued to clarify the role of vanadium species in GLC transformation by using two commercial catalysts: NH_4VO_3 (V^{5+} source) and $VOSO_4$ (V^{4+} source) and two heteropolyacids HPA-1 ($H_4PV_1Mo_{11}O_{40}$) and HPA-5 at 90 °C and 20 bar O_2. At shorter reaction times (3 h) only HPA-5 showed good activity (around 34% FA yield). NMR and EPR spectroscopy were used to monitor the V^{5+} and V^{4+} species, respectively, before and after the reaction. They observe that the HPA-5 solution (catalyst dissolved in the continuous phase) before reaction contained HPAs with higher and lower levels of vanadium substitution. However, after the reaction, only HPA with lower substitutions were detected. The authors concluded that the active species in HPA-5 are the V^{5+} containing HPAs with higher levels of substitution.

On the other hand, Lu et al. [72] studied the impact of solvents on GLC oxidation at 160 °C, 30 bar O_2 and 10 min of reaction time using HPA-2 as catalyst. They found a total selectivity to FA in aqueous solution and 45% of CO_2 in gas phase. Adding 50% v/v of methanol to water reduces CO_2 production to around 4% but also decreases FA yield and selectivity due to the formation of dimethoxymethane and methyl formate. The catalyst behavior was studied by NMR spectroscopy, and it was found that methanol stabilizes the HPA structure, preventing vanadium over-oxidation due to lower VO^{2+} release. The catalyst showed excellent stability in 4 reaction cycles.

A comparative study between several types of HPA was also reported by Voβ and co-workers [74] at 160 °C, 20 bar of O_2 and 1 h of reaction time. The best performance was obtained with HPA-3 catalysts ($H_6PV_3Mo_9O_{40}$) with 36% FA yield and 27% CO_2 yield. Even though FA was the main product in liquid phase, acetic acid and glyceraldehyde formation also took place.

Some iron and manganese compounds were also studied for this reaction as an alternative to the vanadium compounds. A mixture of iron (III) chloride and sulfuric acid ($FeCl_3$–H_2SO_4) was proposed as catalyst by Hou et al. [75]. The reaction carried out at 170 °C and 30 bar O_2 for 50 min, results in full glucose conversion with 53% FA yield in liquid phase and carbon dioxide production. Acetic and glycolic acids were detected as secondary products. The proposed mechanism involves the oxidation of glucose with the reduction of Fe^{3+} to Fe^{2+} deoxidized later by the molecular oxygen.

All the systems described up to now include a reaction in homogeneous phase. However, the use of manganese oxides as alternatives orients the systems toward heterogeneous catalysis. Li et al. [76] studied the effectiveness of 3 manganese oxides. The highest yield of FA 81% was found for MnO_x-100 sample, prepared hydrothermally at 100 °C and tested at 160 °C in 30 bar O_2 and 2.5 h reaction time. The main proposed mechanism of conversion includes glucose α-scission to arabinose as intermediate. However, the catalyst deactivated after three successive runs due to the increased leaching of Mn and decreased surface-adsorbed oxygen. Xu et al. [77] found that bimetallic Mn–Ce oxides provide better activity in comparison to their monometallic oxides attained to the increase of the surface area and corresponding surface-adsorbed oxygen for the mixed samples. The best results were obtained at 160 °C, 30 bar O_2 after 3.5 h, with 63% FA yield over $Mn_4Ce_{0.05}O_x$ catalyst. Another mixed oxide containing manganese and molybdenum was studied by Guo et al. [78]. The highest FA yield of 79%, under reaction conditions (160 °C, 30 bar O_2 for 1.5 h) was achieved for 5% Mo added to MnO_x. A continuous increase of Mo did not result in further improvement due to the decrease of the overall proportion of Mn^{2+} and Mn^{3+} species, suggested as active sites for oxidation. A summary of all described studies including catalysts, solvents and reaction conditions is listed in Table 1.

The oxidation of glucose to formic acid is still a very challenging process from a heterogeneous catalysis point of view. Up to date stable heterogeneous catalysts are still missing, but the nature of the active species oscillates around vanadium, manganese and molybdenum species. The exigency of the direct oxidation process (high oxygen pressure and moderate temperatures) makes difficult the stabilization of the catalytic systems causing severe leaching and giving the main future direction for the process: discovering of a stable catalytic system.

Formic acid is also produced as a byproduct during the synthesis of levulinic acid from biomass. All involved processes and catalysts are frequently reviewed [79–81] and are not the subject of this review. Nevertheless, we will consider the levulinic acid in the next section as a principal substrate for CTH or HDO reactions using formic acid as a natural continuation of the biomass upgrade of co-produced platform molecules.

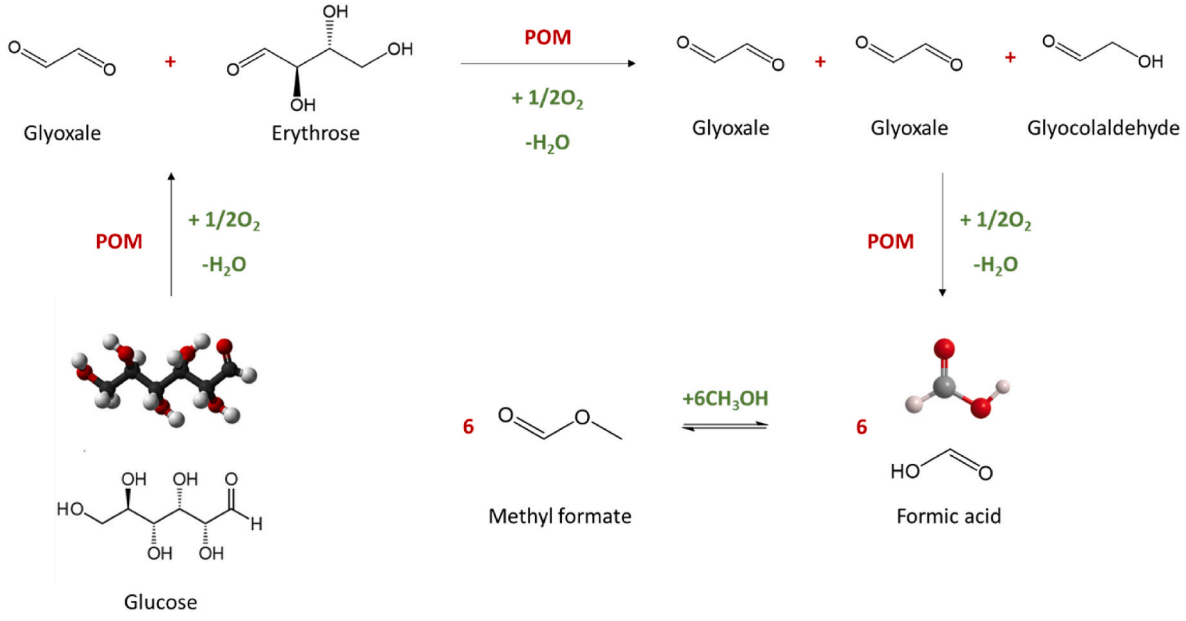

Scheme 4. Glucose oxidation in methanol over polyoxymethylene (POM) based catalysts, adapted from Ref. [72] with permission from Elsevier.

Table 1
Overview of the catalytic systems used for formic acid production from glucose.

Catalyst	Solvent	Oxidant	Conversion %	Yield %	Timeh	Temp °C	Ref.
$Al(OTf)_3$	water	H_2O_2	85	6.8	12	70	[63]
CaO	water	H_2O_2	100	45	0.5	70	[64]
MgO	water	H_2O_2	90.5	78.6	4	50	[65]
HPA@SiO_2–S–N2	water	H_2O_2	78	–	12	70	[68]
hydrotalcite	ethanol	H_2O_2	38.7	5	6	70	[66]
Mg–Al oxide	ethanol	H_2O_2	62	10.2	6	70	[67]
HPA-4	water	O_2	–	25.6	8	90	[69]
HPA-5	water	O_2	53.2	37.8	8	80	[70]
HPA-5	water	O_2	100	55	24	90	[71]
HPA-5	water	O_2	43	34.3	3	90	[73]
HPA-2	50% v/v MeOH	O_2	100	25	0.17	160	[72]
HPA-3	water	O_2	100	36	1	160	[74]
$FeCl_3$–H_2SO_4	water	O_2	100	53	0.83	170	[75]
MnO_x-100	water	O_2	100	81.1	2.5	160	[76]
$Mn_4Ce_{0.05}O_x$	water	O_2	–	63.4	3.5	160	[77]
Mn–Mo oxide	water	O_2	100	79	1.5	160	[78]

3. CTH reactions using formic acid as reagent

3.1. Levulinic acid upgrading

Levulinic acid (LA) has been recognized as one of the top 10 biomass-derived platform compounds [82] and presents an interesting molecular structure (carbonyl (C═O) and carboxyl (-COOH) functional groups). The acid is mainly produced via acid-catalyzed hydrolysis of the LCB and a subsequent dehydration reaction in a low-cost process [83,84]. The starting feedstocks are normally cellulose/C6 sugars via 5-hydroxymethylfurfural (HMF) intermediate [85] or hemicellulose/C5 sugars via furfural (FF) intermediate [86]. Once obtained, LA can be converted into high valuable bio-chemicals, *i.e.* hydrogenated to γ-valerolactone (GVL) [87,88], 2-methyltetrahydrofuran (MTHF) [89], 1,4-pentanediol (PDO) [90], valeric acid (VA, pentanoic acid) [91], oxidized to various organic acids like 3-hydroxypropanoic acid [92], succinic acid [93] etc., or condensed with other molecules such furfural [94], phenols [95] etc. (Scheme 5).

The hydrogenation of levulinic acid to γ-valerolactone is one of the most interesting reactions, due to its specific physicochemical features and prospective fuel applications [96,97]. GVL is considered a safe, biodegradable and nontoxic compound with broad applications as biofuel and fuel additive [98], food additive [99], green solvent [100] or as a platform molecule for a variety of derivatives, including PDO, alkanes, and MTHF [101].

GVL is produced from LA either by hydrogenation with molecular hydrogen at high pressures or by catalytic transfer hydrogenation (CTH) reaction with H-donor compounds. The CTH of levulinic acid with formic acid as internal hydrogen source has been investigated using both homogeneous and heterogeneous catalysts. Our interest in this review will center principally in the CTH reactions with formic acid over noble and non-noble metal based systems as well as over some bimetallic formulations.

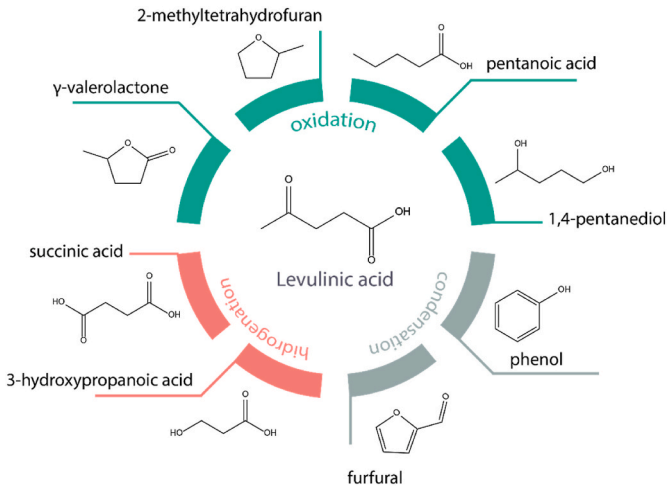

Scheme 5. Levulinic acid platform.

The levulinic acid conversion to γ-valerolactone goes through two possible pathways (Scheme 6) [102]. In the first one, LA is hydrogenated to 4-hydroxypentanoic acid (4-HPA) over metallic sites and further transformed to GVL through cyclization (dehydration) over acidic sites. On the other hand, the second pathway, considered predominant, involves LA dehydration over acidic sites to form an intermediate called angelica lactone (AGL) which is subsequently hydrogenated to GVL over metallic sites. No matter the pathway, the presence of acidic sites promote some secondary reactions such as LA polymerization and coke formation [103]. After GVL the upgrade can continue resulting in pentanoic acid after isomerization and hydrogenation or to methyl tetrahydrofuran (2-MTHF) after hydrogenation and dehydration.

3.1.1. Noble-metal based catalytic systems

Ru-based catalysts were among the most employed in LA to GVL catalytic transformation. Deng et al. [14] evaluated the performance of $RuCl_3{\cdot}3H_2O/PPh_3$ mixture (0.2/0.6 M ratio) as catalyst at 150 °C and 12 h of reaction time using 1 equivalent of formic acid. The authors compared the effect of various bases (KOH, NaOH, Et_3N, pyridine, NH_3, LiOH) on GVL yield and they found that the use of Et_3N and pyridine resulted in very high yields (94% and 93%, respectively). Similar yields have been obtained after shortening the reaction time (6 h) but at higher temperature (200 °C) using the same Et_3N and pyridine bases. The same reaction, in aqueous media using various ligands (PPh_3, dppe, tppms, tppts and PCy_3) and under the initial reaction conditions (150 °C, 12 h and 25 mL of water), showed important GVL yields within the 80–90% range, being the PPh_3 the most beneficial ligand.

In another study of the same group [106], $RuCl_3$ was immobilized on functionalized silica resulting in three different samples (Ru–N/SiO_2, Ru–S/SiO_2, Ru–P/SiO_2 with N═NH_2, S═SH, P═ PPh_2). The highest GVL yield (96% at 150 °C, 12 h reaction time) resulted for Ru–P/SiO_2 catalyst performing as bifunctional catalyst for FA dehydrogenation and LA hydrogenation. Nevertheless, the recyclability tests showed an important decrease in GVL yield (43%) after 3 runs attained to the reduction of Ru^{2+} species to Ru^0, according to the XPS analysis.

Ruppert et al. [52] investigated the impact of catalyst (Ru/C) preparation method and reduction temperature on its CTH activity. They use two precursors ($RuCl_3$ and $Ru(acac)_3$), and two reduction temperatures: low 200 °C (LR) and high 500 °C (HR). The reaction was carried out in

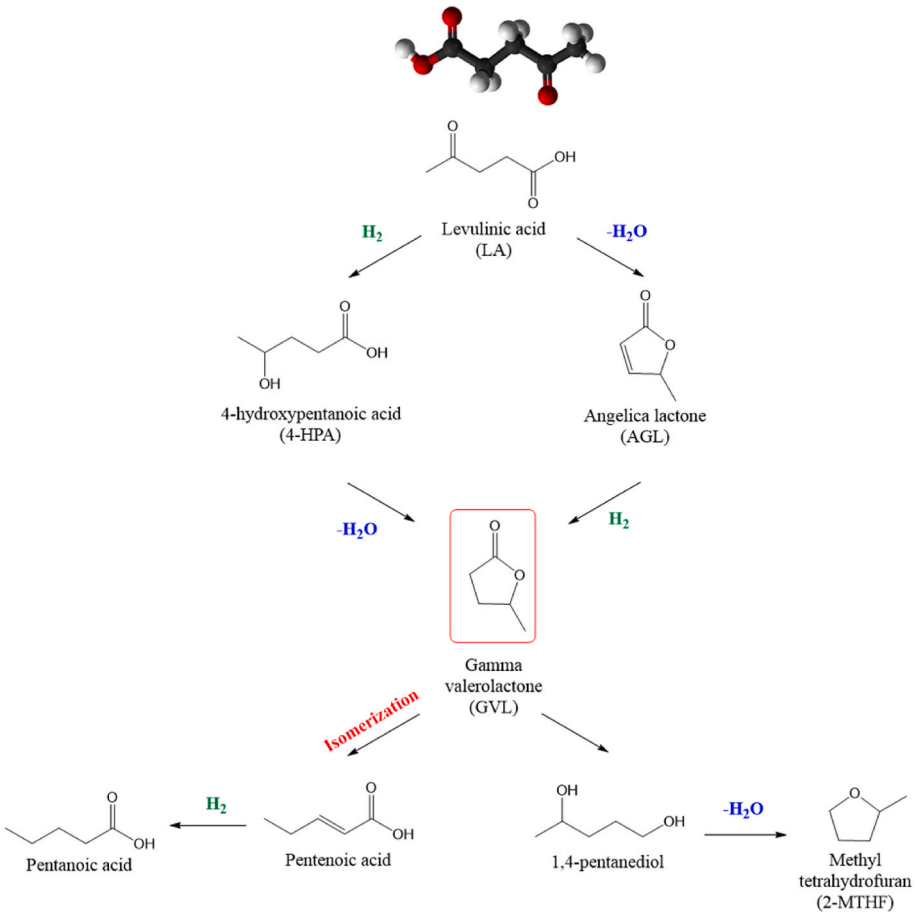

Scheme 6. Catalytic hydrogenation of LA to GVL and subsequent products. Adapted from Refs. [104,105] with permission from MDPI and Royal Society of Chemistry.

aqueous phase at 190 °C for 2 h, being the Ru/C(Cl)HR sample (prepared from $RuCl_3$ precursor by incipient wet impregnation and reduced at 500 °C) the one that achieve a complete formic acid decomposition, high LA conversion (81%) and medium GVL yield (57%). The authors compared the efficiency of Ru/C, Pd/C and Pt/C and explained the higher activity of Ru/C by the decrease of the reaction energy barrier provided by the oxophilic metals (like ruthenium) in aqueous solutions [107].

Feng et al. [108] reported GVL production from LA over Ru (5 wt %)/C, using FA produced from cellulose as hydrogen source in presence of triethylamine (Et_3N). The catalyst showed 87% LA conversion and 81% of GVL yield at 160 °C after 3 h of reaction using 10 g/mol (LA) catalyst and 150 mL/mol Et_3N. They found that an increase of Et_3N leads to an increase in both LA conversion and GVL yield as a consequence of hydrogen formation from the reaction between FA and $E_{t3}N$. Later, it was reported that the addition of Et_3N base facilitates the hydrogen transfer and reduces byproducts formation [14]. However, an excessive amount of Et_3N provokes a slight decline in both LA conversion and GVL yield, suggesting an inhibitory effect in a strongly alkaline environment. The temperature effect was also studied within the 40–180 °C range where the GVL yield slowly increased with the reaction temperature achieving a maximum at 160 °C [109]. Further increase of the temperature caused a decrease of GVL yield to 38%, attributed to multiple side reactions. During the reaction, the formic acid rapidly decomposes to H_2 and CO_2, leading to a reactor pressure increase and system polarity decrease. As a consequence, LA rapidly decomposes in other products since GVL formation remains slow and complex [110].

Gao et al. [111] investigated the performances of Ru/ZrO_2, Ru/TiO_2 and Ru/Al_2O_3 catalysts, using an equimolar formate/formic acid mixture in water at 150 °C in 12 h reaction time. The catalysts were prepared by sol-gel method to trap the ruthenium nanoparticles within the support. The Ru/ZrO_2 catalyst achieved 73% LA conversion and 73% GVL yield with full formic acid/formate decomposition. Nevertheless, Ru/TiO_2 and Ru/Al_2O_3 achieved 98% of FA decomposition with 16% and 0% of LA conversion, respectively. The absence of activity in LA hydrogenation for the latter was attributed to the changes produced after an acid attack (LA or FA) on Al_2O_3 crystallinity [112,113]. Ru-based catalysts supported on various supports (C, SBA-15, Al_2O_3, TiO_2, ZrO_2) have been also reported [114] using water as solvent, equimolar FA/LA ratio at 150 °C for 5 h. Poor LA conversion (10–31%) and GVL yield (2–22%) for all catalysts were detected. Only 5 wt% Ru/C sample showed higher GVL selectivity (73%). Increasing the FA/LA molar ratio to 3 reflected in full LA conversion, 90% GVL yield, but only a 43% of FA conversion.

Fábos et al. [115] reported full LA conversion and 99% GVL yield at 100 °C after 500 min at FA/LA molar ratio = 2 with the use of organo-rhutenium Shvo catalyst, $\{[2,5\text{-}Ph_2\text{-}3,4\text{-}(Ar)_2(\eta^5\text{-}C_4CO)]_2H\}Ru_2(CO)_4(\mu\text{-}H)]\}$ (Ar = *p*-MeOPh, *p*-MePh, Ph, respectively) in an open vessel. Ortiz-Cervantes [116] investigated the catalytic activity of ruthenium nanoparticles in water and water/triethylamine mixture at 130 °C for 24 h being the LA:Et_3N:FA molar ratio 1.0:1.6:5.4. An excellent conversion of LA (99%), high selectivity (100%) and yield (100%) to GVL were obtained with low loading of Ru-NPs (particles size ~5 nm and using $[Ru_3(CO)_{12}]$ as precursor). For the same catalyst, a drastic deactivation was detected, dropping LA conversion to 40% after the 3rd run and with a complete loss of activity in the 4th run. This behavior was attributed to nanoparticles agglomeration. Amenuvor et al. [117] investigated the catalytic performance of a series of pyrazolylphosphite ruthenium (II) complexes in solvent-free condition at

120 °C during 16 h with 0.1 mol% catalyst loading, 20 mmol of FA and 20 mmol of KOH. The neutral catalyst complexes showed 96% LA conversion and 100% GVL selectivity while the rest of precursors presented traces of 4-hydroxyvaleric acid (4-HVA) as intermediate with low LA conversion and GVL selectivity. It was suggested that the neutral catalyst precursors may have higher activity than their cationic counterparts due to the higher stability of the cationic complexes (chelate ring formation).

The addition of base promotes the formic acid deprotonation and dehydrogenation to CO_2 and H_2 [118] and facilitates the coordination of formate ion to the metal center, thus enhancing H_2 heterolysis and in consequence the hydrogenation reaction [119]. In this sense, Oklu et al. [120] reported the performance of pyridylimine ruthenium (II) complexes as catalyst precursors. The catalytic tests were carried out in presence of potassium hydroxide (KOH) or triethylamine (Et_3N) as a solvent at 150 °C during 12 h. The highest yield was found while using Et_3N (100% GVL selectivity and 98% LA conversion) and without formation of 4-HVA as intermediate. In contrast, the KOH promotes the production of 4-HVA intermediate decreasing the LA conversion but showing a full GVL selectivity. The catalyst operated 3 runs without any noticeable loss in activity. The authors demonstrated that their catalysts perform better with organic bases (Et_3N) than with inorganic bases (KOH) and more studies demonstrated that the absence of base lead to low LA conversion with or without catalyst [121].

Another study [122] reported the use of cyclopentadienone Ru^0 complexes with different N- or P- donor ligands for the conversion of equimolar FA/LA mixture at 120 °C after 4 h. The pre-catalyst (as synthesized complex) showed 84% LA conversion with 99% GVL selectivity in EtOH solvent using KOH as base. Prolonging the reaction time up to 16 h lead to LA conversion increase (97% with 99% GVL selectivity). Nevertheless, a longer reaction time (24 h) produced traces of MTHF (7%) decreasing the GVL selectivity. The pre-catalyst showed excellent stability during four cycles without important decrease in activity. Noyori's catalysts (Ru−TsDPEN) were also evaluated in asymmetric transfer hydrogenation (ATH) of LA to GVL with FA [123] in methanol and using N-methylpiperidine (in 1:1 M ratio respect to FA). 98% yield of chiral R-GVL with enantiomeric excess of 93% was obtained at 30 °C after 16 h of reaction time.

Au-based catalysts are also commonly employed in LA conversion to GVL. Son et al. [114] were able to produce a reasonable GVL yield using 5 wt% Au/ZrO_2 catalyst in water at 150 °C during 5 h. The catalyst showed excellent activity and recyclability with full LA conversion, high GVL yield (97%) and complete FA decomposition to CO_2 and H_2. The catalyst activity remained stable for at least five consecutive runs. The same catalyst was used for one-pot synthesis of GVL from fructose under the same conditions showing 48% GVL yield. Du et al. [124] also prepared gold NPs supported on acid-tolerant zirconia (Au/ZrO_2-VS). The catalyst showed full LA conversion with selectivity to GVL rounding 99% at 150 °C after 6 h of reaction at LA/FA molar ratio = 1. The material demonstrated important stability in five runs with an insignificant GVL yield decrease to 95%. The authors evaluated the support nature effect on this reaction. While Au/TiO_2 sample showed moderate GVL yields, Au/SiO_2 and Au/C catalysts were almost inactive, leading to traces of desired product. On the other hand, Li et al. [125] investigated the performance of Au nanoparticles supported on $Ce_xZr_{1-x}O_2$ mixed oxides in aqueous media and equimolar FA/LA mixture. The best results were registered for 2 wt% $Au/Ce_{0.4}Zr_{0.6}O_2$ sample with 91% LA conversion and 83.5% GVL yield at 240 °C after 2 h. At prolonged reaction times, LA conversion increased slightly but the associated GVL yield and selectivity decreased significantly in favor to methyltetrahydrofuran (MTHF). Activity loss was not observed after five runs (90% LA conversion) attributed to both, improved metal-support interaction in presence of Ce [126], formation of tetragonal zirconia phase [127] stabilizing Au against leaching in acidic conditions. In another study [128], several supported Au NPs (Au/ZrO_2, Au/C, Au/Al_2O_3, Au/SiO_2, Au/TiO_2, Au/MgO) were evaluated at 210 °C during 5 h. The 6 wt% AuNPs/ZrO_2-D catalyst (prepared by co-precipitation method) showed the best catalytic results, reaching 93% of LA conversion and 85% GVL yield. The authors suggested the existence of Au^{3+} species involved in GVL yield improvement. Species leaching caused GVL yield decrease to 69% after three successive runs.

On the other hand, Al-Naji et al. [129] studied the catalytic performance of Pt nanoparticles supported on mesoporous zirconia (Pt/MP-ZrO_2). The catalyst showed 97% LA conversion and 90% GVL yield at 240 °C in 24 h with complete FA conversion to H_2 and CO_2. However, the efficiency drops importantly after 4 reaction cycles. At high reaction temperature (above 240 °C), the reaction equilibrium shifted from GVL to pentanoic acid (PA) formed with 22% yield after 24 h of reaction time. Ortiz-Cervantes et al. [118] investigated the efficiency of palladium complexes. The pre-catalyst [(dtbpe)$PdCl_2$] showed complete LA conversion and GVL yield at 100 °C, 1 h, 1 equivalent of FA, 33 mol.% of NEt_3 in water and 0.1 mol.% of Pd complex. The change of the solvent resulted in poor GVL yields, 9% for 1,4-dioxane and 3% for THF. The highest activity in water medium was related to the higher decomposition capability of [(dtbpe)$PdCl_2$] in aqueous media [130].

3.1.2. *Non-noble metal based catalytic systems*

Nickel, copper and iron-based systems are the most studied non-noble catalysts. Varkolu et al. [131] studied Ni dispersed on various supports (MgO, Al_2O_3 and hydrotalcite) as catalysts for the gas phase hydrogenation of levulinic acid. Within the series, Ni/Al_2O_3 showed the best catalytic results converting 99% of LA to GVL yield up to 90% at 250 °C and 1 h of reaction. They found that the main factors related to Ni/MgO deactivation were both, water and coke formation during the hydrogenation and condensation reactions, respectively, as reported also by Mohan et al. [132]. In another study from Varkolu's group [133], Ni/SiO_2 catalyst prepared by citric acid assisted method achieved complete LA conversion and 93% GVL yield in the reaction conditions reported above. The conversion continuously decreased with the time on stream attributed to catalyst' coking activity increase in presence of formic acid. The latter acts as Brønsted acid catalyzing the condensation of reaction intermediates and leading to coke formation. Therefore, the CTH reaction in liquid phase must solve the main challenge of preventing the catalyst deactivation. Gundekari et al. [134] studied the catalytic transfer hydrogenation of LA to GVL over Ni/SiO_2–Al_2O_3 catalysts in a batch reactor using water as solvent. The catalyst shows 70% LA conversion with 70% GVL yield at 200 °C in 10 h of reaction. Guo et al. [135] reported the use of Ni-functionalized carbon (Ni/NiO-FC) in ionic liquid 1-butyl-3-methylimidazolium chloride ([BMIM]Cl) as solvent and super critical CO_2 ($scCO_2$-IL) with FA/LA molar ratio of 12. They found 98% of LA conversion and 97% GVL yield at 170 °C after 3 h of reaction time. Nevertheless, the use of such FA/LA ratio could produce an excess of hydrogen leading to further GVL hydrogenation into byproducts and lowering lactone selectivity [115,136]. On the other hand, the formation of byproducts lowers the reaction phase viscosity promoting the mass transfer and therefore the hydrogenation reaction. In addition, catalyst recycling showed acceptable stability with 5% of catalytic activity loss after five catalytic cycles.

Yuan et al. [13], investigated the performance of Cu/ZrO_2–OG catalyst (OG stands for oxalate gel preparation) achieving complete LA conversion and GVL yield at 200 °C after 5 h of reaction in batch reactor. Some reports argued the use of supported copper catalysts in hydroconversion of carboxylic acids due to Cu leaching [14] and subsequent deactivation, but the 20 wt% Cu/ZrO_2–OG catalyst showed high stability. No copper ions were detected after catalyst recycling, suggesting strong metal-support interaction between copper and zirconium oxide matrix [137] and complete absence of metal leaching. In addition, the XRD results showed no important change in Cu NPs mean diameter after recycling. Lomate et al. [138] used commercial Cu–SiO_2-Q6 catalyst (average pore diameter of 2.9 nm) in a fixed bed reactor, obtaining 66% LA conversion and 81% GVL selectivity at 270 °C after 1 h of reaction. They suggested that Cu^+ species act as Lewis's acid sites, forming angelica lactone (AGL) via dehydration [139]. Another study of the same

group [140] evaluated several supported copper catalysts (Cu–SiO_2, Cu–TiO_2, Cu-ZSM-5, Cu–Al_2O_3 and Cu-SAL), with a copper loading of 6 wt% each. Among them, Cu–SiO_2 showed good performance with an increase of LA conversion (48 vs. 56%) and GVL selectivity (80 vs. 87%) with the increase of FA concentration (1:2 to 1:3 LA/FA ratio). Cu–Al_2O_3 showed a good selectivity toward GVL, but a low LA conversion; while Cu-ZSM-5, Cu–TiO_2 and Cu-SAL catalysts exhibited high selectivity toward AGL attributed to the presence of acidic sites. Cu–TiO_2 showed the highest selectivity to pentanoic acid and the lowest LA conversion and GVL selectivity.

The intrinsic magnetic properties of iron oxides have attracted attention, providing an easier catalyst separation step after reaction. Ashoukraju et al. [141] evaluated the performance of Cu/Fe_2O_3 catalyst under optimized conditions (250 °C, 1 h) in down-flow fixed bed glass reactor. The LA conversion and GVL selectivity linearly increased with the copper content, although some decrement in conversion was detected after 8 h of time on stream. More reports over the same system assumed that LA transformation depends on copper and iron oxide particles presence [142–145]. While iron oxides particles decompose selectively FA [146], a moderate LA conversion is observed over pure Fe_2O_3 catalyst suggesting that the hydrogenation role is played by the copper metal. Yepez et al. [145] evaluated also supported iron oxide nanoparticles on porous silicates. The prepared Fe/Zr-SBA-15 showed a low LA conversion (30%) with 78% GVL selectivity at 200 °C after 1 h of reaction in pressure-controlled CEM-Discover microwave reactor. Homogeneous catalysts were employed by Godwa et al. [147], particularly earth-abundant metal carbonyls M − CO (with M: Fe, Co, W, Cr and Mo) nanoparticles. $Fe_3(CO)_{12}$ pre-catalyst achieved 93% of GVL yield at 190 °C in aqueous media with FA/Et_3N molar ratio = 6:1 after 36 h of reaction.

As an alternative to Ni and Cu based systems, several MnCo oxide catalysts have been reported [148], being the $Mn_2Co_{0.1}O_x$ formulation the one that provided the best results (around 79% LA conversion and 77% GVL selectivity at 230 °C after 20 h of reaction in aqueous medium and FA/LA molar ration of 10). Byproducts have also been observed, valeric acid being the principal, but also acetone, ethanol, isopropanol and even methane. It was suggested that the lattice distortion of $MnCoO_3$ phase lowers the overall reaction energy barrier by favoring the formation of H–H bond between two adjacently pre-adsorbed H atoms on the catalyst surface. In that way, the hydrogen desorption step results favored, increasing the rate of hydrogenation reaction [149–151]. The presence of Co promotes the π-π interaction with the ketone group of LA [152], while Mn species enhance the C–H bond cleavage rate thus promoting H_2 generation [153–155]. In addition, MnCo catalysts presented excellent recyclability after five cycles without any significant loss in activity.

3.1.3. Bimetallic catalytic systems

Bimetallic catalyst formulations have received important attention in LA CTH reaction due to the presumption that the combination of the properties of two metals could influence both hydrogen generation reaction and following hydrogenation. Drew et al. [156] used bimetallic 15 wt% RuRe/C catalyst achieving 95% LA conversion and 95% GVL selectivity. Complete FA conversion was attained in presence of sulfuric acid at 160 °C. Nevertheless, these drastic conditions caused a severe deactivation of the monometallic Ru/C counterpart. Sneka-Platek et al. [26] reported the use of Ag–Pd bimetallic catalysts prepared by different impregnation methods (co-impregnation method (CIMP), subsequent impregnation method (SIMP), co-impregnation method with chemical reduction (CIMPCR) and subsequent impregnation with chemical reduction (SIMP-CR). A 4%Ag–1%Pd/AlOOH catalyst prepared by the four methods reached a complete formic acid decomposition at 190 °C after 2 h but the LA conversion and GVL yield remained low, 34% and 32%, respectively. All the other catalysts showed very low LA conversion and GVL yield. Serra et al. [157] investigated the catalytic activity of Ni–Pt mesoporous nanowires (MNWs) at 140 °C for 2 h in free-solvent conditions and LA/FA weight ratio of 1/2. Ni–Pt MWs showed an excellent performance with GVL yield up to 99% and complete LA conversion. Notwithstanding, only the $Ni_{78}Pt_{22}$ showed excellent reusability, with minimal nickel leaching into the reaction mixture. The catalyst operated in 4 successive cycles without loss of activity or need of catalyst reactivation. The increase of the Ni content, however, resulted in an important metal corrosion.

Bimetallic 1%Au– 2%Ni/ZrO_2 catalyst have been reported by Zhou et al. [158] using equimolar FA/LA mixture, achieving 89% LA conversion and 88% GVL yield (complete FA decomposition) in aqueous solution at 240 °C and 1 h of reaction. Longer reaction time did not appear to impact the process; though increasing the temperature up to 260 °C lead to a slight decrease in GVL selectivity due to its further hydrogenation to pentanoic acid. The authors also studied the performance of monometallic 1%Au/ZrO_2 and 2%Ni/ZrO_2 catalysts separately. The former showed complete FA decomposition for 73% LA conversion and 67% of GVL yield, whereas the latter manifested negligible LA (1%) and FA (19%) conversion.

Soszka et al. [159] evaluated the influence of Ni doping by low noble metals (Pd, Pt, Rh, Ru) amount using water as solvent at 190 °C and 4 h of reaction. The authors found an excellent Ni–Pd activity, 83% LA conversion, full FA decomposition and 79% GVL selectivity. Later work of the same group based on Au–Ni/Al_2O_3 catalysts [27] studied the impact of the preparation methods (subsequent impregnation (SI), deposition precipitation (DP), co-impregnation (CI) and chemical reduction (CR)) on the reaction. Au–Ni $_{(CI)}$/γ-$Al_2O_{3(C)}$ catalyst reached 89% LA conversion and 86% GVL yield with complete FA decomposition at 190 °C in 2 h of reaction. The authors also provided a DFT comparison of the bimetallic Au–Ni alloy with the monometallic Au and Ni formulation and found the existence of strong Au–Ni interaction lowering the energy barrier for FA decomposition. The highest hydrogen production for the bimetallic catalysts resulted in higher GVL yields.

The performance of nickel-promoted copper-silica nanocomposite was investigated by Upare et al. [160]. Within the prepared series, Ni_{20}–Cu_{60}/SiO_2 catalyst showed a complete LA conversion with 98% GVL yield at 265 °C after 10 h of reaction using 1,4-dioxane as solvent and FA/LA ratio of 0.5. The catalyst reached 200 h of operation without deactivation.

Bimetallic Ag–Ni/ZrO_2 catalysts prepared by co-precipitation were also reported [136]. The 10%Ag–20%Ni/ZrO_2 sample achieved a complete FA conversion, 99% LA conversion and 99% of GVL yield at 220 °C after 3 h of reaction in aqueous phase with FA/LA molar ratio of 10. The monometallic formulations (20% Ni/ZrO_2 and 10% Ag/ZrO_2) achieved high GVL selectivity but low GVL yield (22% for Ag vs 34% for Ni).

As reflected above, the CTH reaction using formic acid as H-donor can occur over different metals formulation. While the use of noble metals requires lower temperatures, the non-noble metals need in general 100 °C more and longer times to achieve acceptable GVL yields. The CTH reaction is conditioned by the FA decomposition and higher metal loading is applied in the case of non-noble metals to reach the needed pressure for the subsequent hydrogenation. The variation of the conditions does not allow a proper comparison between the used systems and often very controversial conclusions are made on catalyst stability and deactivation behavior. A summary of the described systems, reaction conditions and results are provided in Table 2.

3.2. Oxygenated furans upgrading via CTH and hydrodeoxygenation reactions

Formic acid can be used in the upgrade of other molecules, all belonging to the biomass feedstock spectra and two of the most important being 5-hydroxymethyl furfural (HMF) and furfural (FF), respectively.

3.2.1. HMF upgrading

HMF can be used to produce a wide variety of chemicals and

Table 2
Formic acid as hydrogen donor in catalytic transfer hydrogenation of levulinic acid.

Catalysts	Solvent[a]	Conversion (%)	Yield[b] (%)	Time (h)	Temperature (°C)	Ref.
Ru/C	Et_3N	87.26	80.75	3	160	[108]
Ru/C	H_2O	81	57	2	190	[52]
Ru–P/SiO2	H_2O	–	96	12	170	[106]
$RuCl_3,3H_2O/PPh_3$	–	–	94	12	150	[14]
Ru/ZrO_2	H_2O	73	73	12	150	[111]
Ru/C	H_2O	100	90	5	150	[114]
Ru-NPs	$H_2O + Et_3N$	99	100	24	130	[116]
Pyrazolylphosphite ruthenium	–	96	100	16	120	[117]
Pyridylimine Ru (II) complexes	Et_3N	98	98	12	150	[120]
Shvo catalyst	–	100	99	8	100	[115]
Ru^0 complexes	EtOH	84	99[b]	4	120	[122]
Ru-TsDPEN	MeOH	99	98	16	30	[123]
Au/ZrO_2	H_2O	100	97	5	150	[114]
Au/ZrO_2-VS	–	100	99	6	150	[124]
$Au/Ce_xZr_{1x}O_2$	H_2O	90.8	83.5	2	240	[125]
Au NPs/ZrO_2-D	–	93.3	85	5	210	[128]
Au–Ni/ZrO_2	H_2O	89.1	87.9	1	240	[158]
Pt/MP-ZrO_2	–	97	90	24	240	[129]
$[(dtbpe)PdCl_2]$	H_2O	100	100	5	100	[118]
Ni/Al_2O_3	–	99	>90	1	250	[131]
Ni/SiO_2	–	100	93	1	250	[133]
$Ni/SiO_2–Al_2O_3$	H_2O	70	70	10	200	[134]
Ni/NiO-FC	$scCO_2$-IL	98	97	3	170	[135]
Cu/ZrO_2–OG	H_2O	100	100	5	200	[13]
Cu–SiO_2-Q6	–	66	81[b]	1	270	[138]
Cu–SiO_2	–	56	87[b]	1	250	[140]
Cu/Fe_2O_3	–	100	100	1	250	[141]
Fe/Zr-SBA-15	–	30	78[c]	1	200	[145]
$Fe_3(CO)_{12}$	–	–	93	36	190	[147]
$Mn_2Co_{0.1}O_x$	H_2O	78.9	76.7[b]	20	230	[148]
RuRe/C	H_2SO_4	95	95[b]	–	160	[156]
Ag–Pd/ALOOH	–	34	32	5	190	[26]
Ni–Pt	–	100	99	2	140	[157]
$Au–Ni/Al_2O_3$	H_2O	89	86	2	190	[27]
Au–Ni/ZrO_2	H_2O	89.1	87.9	1	240	[158]
Ni–Pd(Cl)/γ-Al_2O_3	H_2O	83	79	4	190	[159]
Ni–Cu/SiO_2	DO	100	98	10	265	[160]
Ag–Ni/ZrO_2	H_2O	99	99	3	220	[136]

[a] **Et_3N**: Triethylamine, **EtOH**: Ethanol, **MeOH**: Methanol, **$scCO_2$-IL**: Super critical carbon dioxide and ionic liquid, **H_2SO_4** sulfuric acid, **DO**: 1,4-dioxane.
[b] Selectivity.

biofuels, including levulinic acid [85], 2,5-furandicarboxylic acid (FDCA) [161], ethyl levulinate [162], and 2,5-dimethylfuran (DMF) [163]. Nevertheless, HMF is known as an unstable molecule, participating in unwanted side reactions with the formation of different byproducts besides being transformed by traditional routes [164,165]. That is why, HMF conversion to other value-added products must be undertaken on selective catalyst using formic acid via CTH/HDO/hydrogenolysis reactions. An example of such process is the production of DMF via selective hydrodeoxygenation of renewable HMF [166]. DMF molecule possesses advantageous physical and chemical characteristics to be used as possible liquid transportation biofuel such as a volumetric energy density of 30.0 MJ/L(very close to gasoline), nearly optimal boiling point, miscible with gasoline and immiscible with water. DMF has been already favorably tested in combustion engines [167]. Moreover, DMF can be used as feedstock for the manufacture of *p*-xylene via Diels-Alder reaction [168]. Hence, the production of liquid fuels and chemicals in the future will rely heavily on the reductive upgrading of HMF to DMF. The tests with pure DMF, DMF/gasoline mixtures, and DMF/diesel blends, respectively, are being explored to learn more about their combustion and emission properties for future use in internal combustion engines [169–171]. A complete hydrogenation of HMF can also result in 2,5-Bis(hydroxymethyl)tetrahydrofuran (BHTF) [172], an important compound used in the production of resins, crown ethers, and heat insulating materials [164,173,174]. Furthermore, BHTF is a potential diol that can be used to synthesize memory-shape and self-healing polymers as well as 1,6-hexanediol, another crucial polymer precursor [175].

There are two known pathways for the synthesis of DMF (Scheme 7), the first involves the 5-HMF hydrogenolysis to 5-methylfuran (5-MF) which further hydrogenates to 2-hydroxymethyl-5-methylfuran (HMMF), the latter converted to DMF through hydrogenolysis of its carbonyl group. In the second pathway HMF is hydrogenated to 2,5-bis (hydroxymethyl)furan (BHMF), further converted to HMMF by hydrogenolysis and subsequently transformed to DMF.

Therefore, the synthesis of DMF needs hydrogenation/hydrodeoxygenation catalysts able to activate hydrogen production *in situ* from formic acid. Mitra et al. [172] studied the hydrodeoxygenation of HMF to DMF using FA as hydrogen donor. They used a Pd/C catalyst and achieved 95% HMF conversion and 95% DMF yield, at 120 °C after 15 h using dioxane as solvent. The same catalyst was explored in another study in THF/H_2SO_4 mixture [176], showing complete HMF conversion and 95% DMF yield after 5 h at 110 °C.

Bifunctional Pd NPs supported on N-doped mesoporous carbon (Pd/NMC) has also been reported [177] with 61% of HMF conversion and 39% DMF yield. The nitrogen content appears to promote the activity as the N-free mesoporous carbon supported catalyst (Pd/CMC) reached only 21% of HMF conversion and 13% DMF yield at 160 °C after 3 h in THF solvent. Both catalysts showed important improvement in activity when the FA was combined with gaseous H_2. Pd/NMC achieved full HMF conversion and 97% DMF yield, while the Pd/CMC showed 99% HMF conversion and 72% DMF yield.

Pd–Au/g-C_3N_4 has also been investigated [178], showing good activity with an important DMF yield (86%) achieved in water/ethyl acetate mixture after 1 h at room temperature. The same metals supported

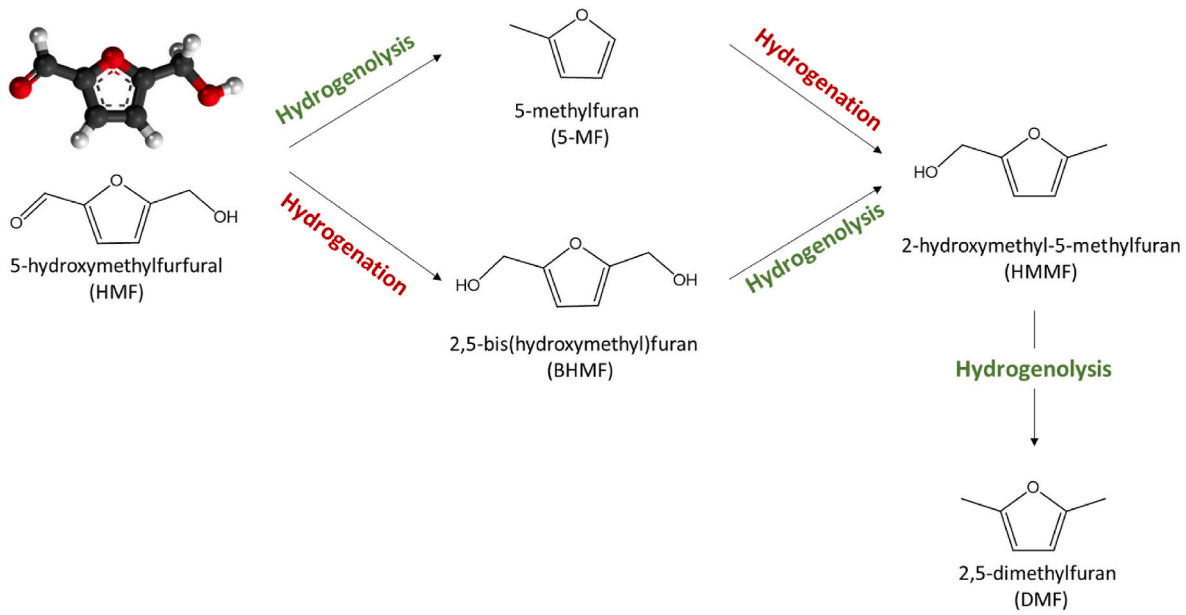

Scheme 7. Catalytic hydrogenation/hydrogenolysis of 5-HMF to 2,5-DMF.

on zirconia were studied by Tao et al. [179] in 1,4-dioxane solvent, reaching 99% HMF conversion and 98% DMF yield after 1.5 h at 140 °C.

The non-noble CoFe-111 catalyst [180] showed also an important DMF yield (90%) and HMF conversion under optimized conditions (240 °C, 2 h reaction time in THF medium) and very good stability after 4 runs without considerable loss in activity. On the other hand, Yang et al. [181] investigated the activity of bimetallic Ni–Co/C catalyst. 2% Ni–20%Co/C catalyst achieved 99% HMF conversion and 90% DMF yield (accompanied with some 5-MF) in THF medium at 210 °C after 24 h of reaction time. The use of molecular hydrogen in the same conditions results in a much lower DMF yield (61%). The formation of 2,5-hexanediol was also observed and increased with the nickel loadings reaching 20% for the 7%Ni catalyst. The recycling tests showed constant HMF conversion in 4 cycles, but a change in selectivity, the DMF yield decreased in favor to 5-MF due to metal leaching. Bimetallic Ni–Cu/C has also been tested [182], and a 10%Ni–10%Cu/C catalyst prepared by incipient wetness impregnation showed full HMF conversion with 80% yield of DMF after 6 h at 200 °C in isopropanol medium.

The catalytic transfer hydrogenation of HMF to BHMF was studied by Thananatthanachon et al. [183] in presence of FA (HMF/FA = 1, in 5 mL THF, 40 °C) over 0.1 mol% Ru catalyst ((cymene)Ru- (TsDPEN)) and 0.5 mol% of iridium catalyst (Cp*Ir(TsDPEN-H) (Scheme 8). Both catalysts achieved 99% of BHMF in 1 or 2 h reaction time. The Ir based catalysts were also active in furfural (FF) upgrade to furfuryl alcohol (FFA) in presence of 10 equivalents of Et_3N using formic acid as H-donor (6 h, 150 °C, 0.1 eq. FA).

The CTH reaction of HMF to 2,5-furandimethanol (FDM) is recognized as a useful reaction to produce building blocks for the biopolymer industry and macromolecules synthesis [184,185]. Xu et al. [186] reported this reaction over stable Co confined catalyst on mesoporous N-doped carbon (Co–NC-A) showing 88% HMF conversion and 86% FDM yield at 160 °C after 5 h in 1,4-dioxane. On the other hand, Tuteja et al. [187] investigated palladium supported zirconium phosphate catalyst (Pd/ZrP) in the hydrogenolysis of HMF to 1,6-hexanediol using formic acid as hydrogen donor and EtOH as solvent. The highest 1, 6-hexanediol yield (42.5%) was obtained over 7 wt% Pd/ZrP, with nearly complete HMF conversion in 21 h at 140 °C.

5-formyloxymethylfurfural (FMF) is another furan compound analogue to HMF with –OOCH replacing the –OH, produced from HMF and chloromethyl furfural (CMF) [188,189], that can be used to produce DMF. FMF has interesting properties including low polarity, high stability, and enhanced hydrophobicity, which facilitates its separation from the reaction mixture using vacuum distillation [188–190]. Sun et al. [190] studied the HMF and FMF hydrogenolysis/hydrogenation with formic acid to produce DMF in THF solvent over mono Ni- or bimetallic Ni–Cu/SBA-15 catalyst. Using FMF as substrate resulted in higher DMF yield in 5 h at 220 °C than using HMF with a slight decline in DMF selectivity after 6 consecutive runs. Similarly, a summary of the described systems, reaction conditions and results are provided in Table 3.

3.2.2. *Furfural upgrading*

Furfural (FF), a key ingredient of bio-oil, is generally produced by acid catalyzed dehydration of pentose-derived sugars such as xylose and arabinose [191]. It is recognized as one of the top 10 biorefinery building chemicals [192] with growing market expectations in the next

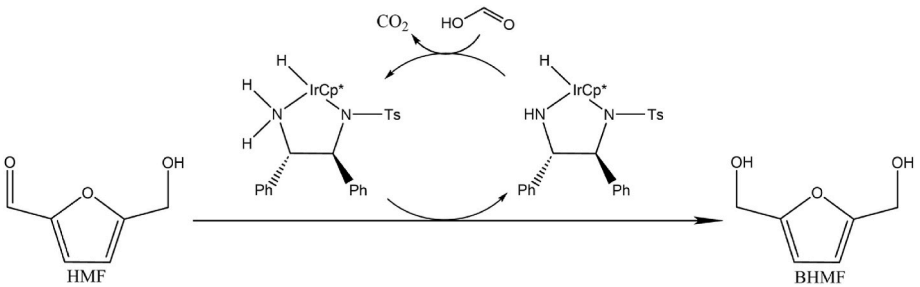

Scheme 8. CTH process of HMF using Cp*Ir(TsDPEN) catalyst with formic acid as hydrogen source, adapted from Ref. [183] with permission from Wiley-VCH.

Table 3
Formic acid as hydrogen donor in the catalytic transfer hydrogenation of HMF.

Desired Product[a]	Catalysts[b]	Solvent[c]	Conversion (%)	Yield (%)	Time (h)	Temperature (°C)	Ref
DMF	Pd/C	DO	95	95	15	120	[172]
DMF	Pd/C	THF + H_2SO_4	100	95	15	110	[176]
DMF	Pd/NMC	–	60.8	39.1	3	160	[177]
DMF	Pd/CMC	–	62.9	13.5	3	160	[177]
DMF	Pd–Au/g-C_3N_4	H_2O/EA	–	99	1	RT	[178]
DMF	Au–Pd/t-ZrO_2	DO	99	98	1.5	140	[179]
DMF	48Ni/SBA-15	THF	100	58.8	5	220	[190]
DMF	CoFe-111	THF	100	92	2	240	[180]
DMF	Ni–Co/C	THF	99	90	24	210	[181]
DMF	Ni–Cu/C	i-PrOH	100	80	6	200	[182]
HDO	Pd/$ZrPO_4$	EtOH	97	43	21	140	[187]
FDM	Co–NC-A	i-PrOH	88.2	86.0	5	160	[186]
BHMF	Cp*Ir(TsDPEN)	THF	100	99	2	40	[183]
DMF	Ni–Cu/SBA-15	THF	100	71	5	220	[190],[d]

[a] **DMF**: 2,5-dimethylfuran, **HDO**: 1,6-hexanediol, **FDM**: 2,5-furandimethanol, **BHMF**: 2,5-bis(hydroxymethyl)furan.
[b] **NMC**: N-doped mesoporous carbon, **CMC**: N-free mesoporous carbon, g-**C_3N_4**: graphitic carbon nitride.
[c] **DO**: 1,4-dioxane, **THF**: Tetrahydrofuran, **H_2SO_4**: sulfuric acid, **EA**: Ethyl acetate, **i-PrOH** isopropanol, **EtOH:** ethanol.
[d] **FMF**: 5-formyloxymethylfurfural was used as substrate in this work.

decades [193], due to its high reactivity and adaptability [82,194]. Several studies have been carried out to convert it into molecules such as furfuryl alcohol (FFA, Scheme 9), furan, 2-methylfuran (2-MF), tetrahydrofuran (THF), cyclopentanone (CPON), etc. [195].

Furfuryl alcohol (FFA) is a useful chemical intermediate, frequently employed in the production of resins, synthetic textiles and fine chemicals [196,197]. Recently, the CTH of furfural to furfuryl alcohol with formic acid as hydrogen donor has been reported over diverse catalytic systems. Ru/C was proposed [198] for the hydrogenation of FF to FFA with formic acid in water/THF mixture (v/v = 1:19) and FF/FFA molar ratio of 1:2. In presence of 10 mol.% of NaOH respect to FF, complete FFA selectivity and almost complete FF conversion were achieved at 90 °C in 6 h of reaction. An increase in temperature up to 110 °C did not significantly improve FF conversion, nor did it enhance FFA selectivity. In another study [199], Rh NPs supported on diamine functionalized KIT-6 (Rh/ED-KIT-6) were employed in 2-propanol medium, but this time, GVL was produced with an excellent yield of up to 97% at 100 °C after 5 h. The catalyst also showed a good stability since any significant loss in activity was observed in 3 runs. On the other hand, Nagaiah et al. [200] studied the CTH of FF to FFA with FA over a 15%Cu/$MgAl_2O_4$ catalyst prepared by impregnation method. The catalyst reached 90% conversion and 99% selectivity to FFA at 210 °C after 13 h of reaction with molar ratio FF:FA = 1:7. The same reaction was studied by Du et al. [201] over a bimetallic Pd–Cu/C catalyst in 1,4-dioxane medium with FF/FAL molar ratio = 1:4. The catalyst showed a complete FF conversion and 98% FFA yield at 170 °C in 3 h and maintained its activity during 5 successive runs. It was suggested that the palladium-based catalysts decompose selectively FA to produce H_2 under mild conditions [30,202] but remain non-selective for the carbonyl group hydrogenation of the furane ring. On the contrary, the copper-based catalysts are more selective toward carbonyl group hydrogenation [203,204]. An important excess of formic acid shifts the reaction equilibrium toward the formation of 2-[(formyloxy)methyl]furan [189].

Xu et al. [205] applied in the same reaction Co particles supported on N-doped carbon in 1,4-dioxane medium. The catalysts obtained after pyrolysis at 700 °C (Co–N–C-700) showed complete FF conversion and FFA yield at 150 °C after 6 h of reaction. No deactivation was found after 5 cycles which was attributed to the stability of the encapsulated Co in N-doped carbon. Other useful chemical obtained from furfural is 2-methylfuran (2-MF) suitable as fuel additive due to its high-octane number (103 *vs.* 97 of gasoline) and good energy density (28.5 MJ/L vs. 31.9 MJ/L of gasoline) [206]. Fu et al. [207] reported the use of 10% Ni–10%Cu/Al_2O_3 in the conversion of FF to 2-MF via CTH reaction with FA achieving 92% yield of 2-MF in isopropanol at 210 °C after 7 h of reaction. The same group [182] reported the use of the same active phase but supported on carbon (10%Ni–10%Cu/C). The same 2-MF yield was obtained at slightly lower temperatures and longer reaction times (200 °C and 8 h). The results of both studies suggest that the support does not participate actively in the reaction mechanism. The used catalytic systems and reaction conditions of furfural upgrade are summarized in Table 4.

3.3. Other biomass feedstocks upgrading

Although levulinic acid has been widely selected as a model compound for the HDO/CTH of LCB derivates, some other interesting derivates and even raw biomass have been studied as model molecules for these processes.

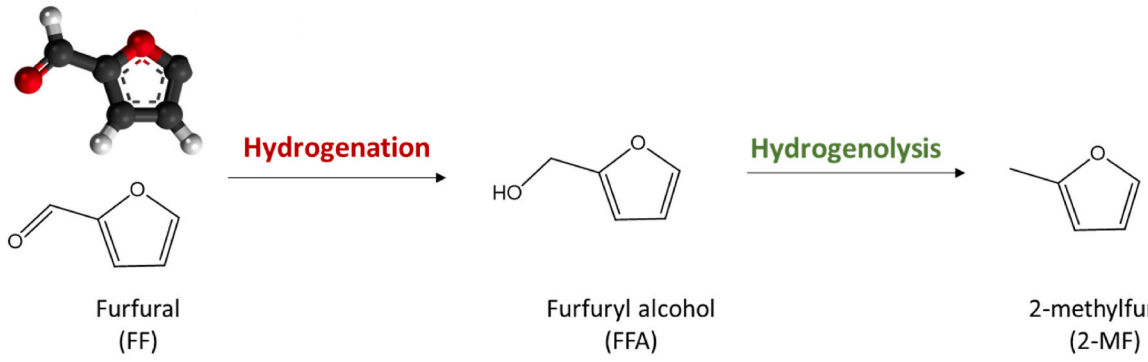

Scheme 9. FF hydrogenation/hydrogenolysis to FFA and 2-MF.

Table 4
Formic acid as hydrogen donor in the catalytic transfer hydrogenation of furfural.

Desired Product[a]	Catalysts[b]	Solvent[c]	Conversion (%)	Yield (%)	Time (h)	Temperature (°C)	Ref.
DMF	Ni–Cu/SBA-15	THF	100	71	5	220	[190]
FFA	Ru/C	THF + H_2O	99.3	99.3	6	100	[198]
FFA	Rh/ED-KIT-6	i-PrOH	98	97	5	100	[199]
FFA	$Cu/MgAl_2O_4$	–	90	99	13	220	[200]
FFA	CuO–Pd/C	DO	100	98.1	3	170	[201]
FFA	Co–N–C-800	DO	97.8	95	6	150	[205]
FFA	Co–N–C-700	DO	100	99.9	6	150	[205]
2-MF	Ni–Cu/C	i-PrOH	100	91	8	200	[182]
2-MF	$Ni–Cu/Al_2O_3$	i-PrOH	100	92	7	210	[207]

[a] **DMF**: 2,5-dimethylfuran, **FFA**: Furyl Alcohol, **2-MF**: 2-methylfuran,.
[b] **ED-KIT-6**: functionalized diamine.
[c] **THF**: Tetrahydrofuran, **i-PrOH**: isopropanol, **DO**: 1,4-dioxane.

3.3.1. Alkadienes

Light alkenes such as ethylene and butenes are some of the most used raw materials in the current organic chemical industry. Petroleum hydrocracking is the main used method of synthesis, generating alkynes and alkadienes as side-products. Products, such as 1,3-butadiene, are reported as catalyst poisoning agents and can provoke detrimental environmental and health issues. Selective catalytic hydrogenation is an effective method proposed to remove these impurities via transforming them into valuable alkenes [208,209]. Carrales-Alvarado et al. [210] studied the selective hydrogenation of 1,3-butadiene to butene on different Pd-supported catalysts. Nanofibers Pyrograph PR24-HHT and PR24-PS and high surface area graphites H100 and H300 are used as supports. A complete conversion is obtained in all cases although higher temperatures are required in the case of nanofibers-supported catalysts. Notwithstanding, and according to the reported TOF values, Pd supported on nanofiber catalysts are slightly more active than graphite supported samples. Higher selectivity towards butenes was observed while using FA instead of molecular H_2, due to small quantities of CO produced and reported to enhance butene selectivity. Graphites supported catalysts produced higher CO quantity and higher butenes yield.

3.3.2. Glycerol

Glycerol is a versatile by-product of an extensive variety of industrial biomass conversion processes such as saponification, sugars fermentation, oils and fats transesterification and biodiesel production. Indeed, it is the latter one that causes an overproduction of glycerol, making its valorization into glycols and alcoholic intermediates critical. Among all possible glycols and alcohols, 1,2-propanediol has become one of the most interesting alternatives since it can be broadly applied in the synthesis of anti-freeze, polyester resins, pharmaceuticals, paints, cosmetics, plasticizers and additives for food and tobacco industry [211,212]. Gandarias et al. [213] evaluated the influence of Ni and Cu supported on Al_2O_3. They observed that glycerol adsorption occurs on alumina acidic sites while Ni catalyzes glycerol hydrogenolysis and Cu enhances the selectivity towards 1,2-propanediol. Once Ni–Cu ratio was optimized, the influence of the hydrogen donor molecule was studied testing methanol, 2-propanol and formic acid. All donor molecules presented important results in terms of glycerol conversion and 1,2-propanediol selectivity as a function of the amount of employed hydrogen donor [212]. The same authors developed a semi-batch system in which the hydrogen donor is constantly pumped into the reactor to prevent the competitive adsorption between glycerol and H-donor molecule that occurs in batch reactor. This system was able to provide an adequate supply of active hydrogen atoms achieving an equilibrium between formic acid and glycerol adsorption and resulting in superior conversion (twice as one obtained in the traditional batch system). On the other hand, Yuan et al. [214] designed stable well-dispersed Cu/ZrO_2 catalyst reaching 94% 1,2-propanediol yield after 18 h at 200 °C. Contrary to the mechanism proposed by Gandarias et al. [212], the authors proposed that instead of a catalyzed transfer hydrogenolysis, glycerol is straightforward hydrogenolyzed by H_2 generated *in situ* by FA decomposition. They believed that the catalyst role of assisting the FA dehydrogenation is the critical factor for the high activity.

Nonetheless, and despite the previous studies pointing FA as the best hydrogen donor for glycerol hydrogenolysis, a recent study by Yfanti et al. [211] proposed methanol as the most effective H_2 donor on Cu:Zn:Al catalyst. They supported that adding both, ethylene glycol and formic acid inhibited the glycerol conversion due to competitive adsorption. Although FA reacts faster than methanol giving H_2, CO_2 and CO, the molecular hydrogen was not able to react with glycerol and desorbed as obtained. In any case, the use of FA appears attractive due to the low quantity (formic acid/glycerol molar ratio) needed for the reaction.

3.3.3. Phenol

The presence of pollutant phenolic compounds in industrial (oil refineries, petrochemical units, coke ovens, polymer resins and plastic manufacturing) or agricultural wastewaters has focused attention on phenol valorization via ring hydrogenation to cyclohexanone [215]. Cyclohexanone is one of the main intermediates of the manufacture of the most used nylon and polyamide resins [216]. Palladium-based catalysts have been used for transfer hydrogenation of phenol. In the work of Zhang et al. [217], for instance, different Pd-supported catalysts were evaluated, mainly activated carbon, basic oxides and metal-organic frameworks (AC, Al_2O_3, TiO_2, TiO_2-AC composite and MIL-101). Firstly, the catalysts series was tested using molecular H_2, designing the metal-organic framework MIL-101 sample as the most active support. However, different results were obtained while using FA as H_2 donor, the Pd/MIL-101 catalyst led to very low conversion. This fact was attributed to a change in mechanism and the competitive adsorption between H_2 donor and acceptor on Pd active sites. Therefore, activated carbon, in which both FA and phenol are moderately adsorbed due to carbon's hydrophobic characteristics, gave the highest activity. It was also observed that the use of FA instead of molecular H_2 provoked a shift in selectivity towards the desired cyclohexanone rather than cyclohexanol.

3.3.4. Carbonyl compounds

The selective reduction of carbonyl compounds has gained interest since primary and secondary alcohols are the main products and key intermediates in the synthesis of many drug molecules and chemicals [218].

Ruthenium encapsulated in aluminium oxyhydroxide-support (Ru/AlO(OH)) was reported as a versatile catalyst for the transfer hydrogenation of both aldehydes and ketones [219]. This method of synthesis ensured very small and uniform metal particles that act as stable and robust catalyst (no leaching observed after five cycles) at low metal loadings (<2 wt%). Ruthenium was also prepared by wet impregnation on Al_2O_3 support ($Ru(OH)/Al_2O_3$) and led to the same conversion though the obtained TOF was lower. Moreover, Ag, Cu and Ni were also supported on AlO(OH) but presented no activity. Focusing on Ru/AlO

(OH), the effect of hydrogen donor was evaluated and compared to molecular hydrogen and potassium formate. The use of molecular hydrogen significantly decreases the conversion (53%) while the combination of potassium formate and catalyst resulted in fast and facile reduction of aromatic and aliphatic aldehydes to a 100% yield. Ketones were not so easily reduced but, after long reaction times, excellent yields were obtained. In addition to ruthenium, iridium and rhodium also present promising and encouraging performances. Wang et al. [220] tested Ir nanoparticles supported on N-doped carbon materials (Ir@CN) in the transfer hydrogenation of aldehydes and ketones. The authors choose 4-methyl benzaldehyde as model molecule and hydrogenate it using molecular H_2 or HCOOH/NaOH mixture over different catalysts: Pd and Ir supported on carbon (Pd/C and Ir/C), Ir nanocatalyst (Ir@CN). Pd/C catalyst was the only active material in direct hydrogenation, while the Ir@CN appeared highly active and selective (99% yield of 4-methylbenzyl alcohol) via transfer hydrogenation. What is more, the Ir@CN catalyst remains stable in 4 cycles attributed to the extremely stable Ir nanoparticles strongly attached to the surface via 1,10-phenanthroline structure. Once again, the hydrogenation of ketones emerged as a more arduous task to achieve, but Ir nanocatalyst achieved a high yield in cyclohexanone-to-cyclohexanol reaction and a moderate yield in the hydrogenation of acetophenone. The last reaction was studied by Sudakar et al. [218] reporting 99% of conversion after 30 h of reaction to 1-phenylethanol as a sole product using also Ir-based catalyst. In this work, an Ir-bypyridine (bpy) complex was incorporated into a covalent triazine framework (CTF) stable in a wide range of temperatures and pressures and in both acidic and basic media. Likewise, CTF provides high surface area, low density and ordered structures. The same procedure was used to synthesize a Rh-bpy-CTF catalyst, which achieved superior activity compared to Ir attributed to the difference in stability of Rh-and Ir-hydride intermediates (the former is less stable than the latter) being Ir more stable upon recycling. In any case, both catalysts showed excellent conversion rates in a large list of aldehydes and ketones.

3.3.5. *Pyrolysis oils*

Although pyrolysis of forestry residues is one of the solutions to produce bio-oil, the produced oil does not always meet the requirements for direct and safe use as fuel. This is the case of Loblolly pine residue oil, difficult to use directly due to thermal instability, high viscosity, corrosiveness, and poor volatility [221]. For that reason, an improvement is required being the hydrogenation the most effective choice of upgrade. A commercial Ru/activated carbon catalyst was used to produce gasoline-range oil from Loblolly pine residue in a two-step process [222]. This FA-assisted hydrogenation achieved the elimination of 78% of the aromatic hydrocarbon content and increase the content of aliphatic hydrocarbons.

3.3.6. *Quinoline*

The product of the quinoline hydrogenation, 1,2,3,4-tetrahydroquinoline (THQ), is an essential intermediate to produce drugs, dyes, alkaloids, agrochemicals and other biologically active molecules [223]. Tao et al. [224] firstly evaluated the performance of small Au nanoparticles supported on acid-tolerant zirconia, finding high activity towards FA decomposition but poor selectivity towards THQ. Then, Au NPs were supported on a single-phase rutile titania resulting in high yields and excellent selectivity towards THQ from quinoline derivatives. Additionally, they established a direct route to obtained N-formyltetrahydroquinoline (FTHQ, molecule with broad use in the pharmacological industry) from quinoline compounds and FA. In other study, Vilhanová et al. [225] used an amino-functionalized silica to support Au NPs. Besides quinoline, they tested fifteen structurally different substrates (all of them N-heterocyclic compounds) reporting high selectivity, high activity and facile catalyst recycling in all cases. Despite the good results obtained with Au the search for non-noble catalyst led Cabrero-Antonino et al. [226] and Li et al. [227] to investigate Co-based catalysts. In the former case, the authors combined $Co(BF_4)_2{\cdot}6H_2O$ with tris(2-(diphenylphosphino)phenyl)phosphine to obtain a selective non-noble catalyst that hydrogenates quinoline without basic additives. This catalyst selectively reduced quinoline in presence of other sensitive functional groups [226]. In the case of Li et al. [227] an ordered mesoporous N-doped carbon (OMNC)-encapsulated Co (Co@OMNC) catalyst was compared to the control catalysts, Co supported on N-doped carbon (without using SBA-15 precursor) and on active carbon. The encapsulated catalyst presented higher and more stable quinoline conversion due to the mesoporous structure since it isolates the Co species from the acidic reaction media avoiding the Co leaching observed for the catalysts prepared by impregnation. Furthermore, the ordered mesoporous structure favored the access of reactants to the active sites with Co@OMNC presenting a superior acid-tolerance, substrates adsorption rate and therefore superior performance.

3.3.7. *Vanillin*

4-hydroxy-3-methoxybenzaldehyde, better known as vanillin, is one of the main components (or at least the most studied) derived from the lignin fraction [228]. Its hydrodeoxygenation product, 2-methoxy-4-methylphenol (MMP, Scheme 10), has been extensively used as intermediate for cosmetics and drugs [178].

Multiple, mono o bi-metallic catalyst formulations have been proposed for the hydrodeoxygenation of vanillin [229]. In this sense, Au, Pt and Au–Pt alloy nanoparticles were supported on CeO_2. While the monometallic catalyst did not show high conversion or selectivity to MMP, the bimetallic combination reached complete vanillin conversion and 99% of MMP selectivity. Supporting Au–Pt alloy on AC and SiO_2 resulted in lower selectivity and conversions than the presented by Au–Pt/CeO_2. The outstanding behavior of this catalyst was attributed to the contribution of the alloy metals and the synergy working in the two steps: FA dehydrogenation and C═O hydrogenolysis. The reaction was also carried out using molecular H_2 instead of FA leading to lower conversion values. The authors indicated that this fact could be related to the poor solubility of gaseous H_2 in a polar water solvent.

Pd supported over mesoporous carbon led to low vanillin conversion enhanced with the incorporation of nitrogen creating nitrogen-enriched highly mesoporous carbons (NMCs) [230]. Pd/NMC catalyst showed a complete conversion and selectivity towards MMP after 3 h of reaction. The tests carried out on Pd supported over SiO_2, Al_2O_3, CB (carbon black) and AC (active carbon) led to poor activity and low MMP selectivity. It was concluded that the high N content and different pore structure of NMC support assures high Pd dispersion creates N-containing defect sites that increase the hydrophilicity of carbons enhancing the hydrodeoxygenation of vanillin. On the other hand, Pu et al. [231] reported for the first time MOF-derived hierarchically porous carbon (HPC) with controlled honeycomb-like morphology N-doped with dicyandiamide obtained after direct pyrolysis. This support was able to disperse, stabilize and isolate the Pd NPs, leading to a >99% MMP yield in the hydrodeoxygenation of vanillin. Due to the hierarchical structure, the high dispersion of Pd sites and favorable hydrophilicity, Pd@HPC-DCD appeared as versatile catalyst for a series of unsaturated hydrocarbons hydrodeoxygenation.

The hydrodeoxygenation of vanillin achieved 99% of MMP yield at room temperature over supported Pd–Au BMNP (bimetallic nanoparticles) on g-C_3N_4 [178]. Water, ethanol and ethyl acetate were evaluated as solvents. The use of one single solvent or the combination of water/ethanol do not lead to any reaction, suggesting the use of two-phase immiscible solvents. The catalyst action in water/ethyl acetate (volume of EA to $H_2O = 3$) biphasic solvents led to excellent results without any need of protective atmosphere or additives use. Completely different approach used Smith et al. [228] for the heterogenization of Ir homogenous complex on a Merrifield resin (IrPYA). They succeed to produce 54% yield to 4-hydroxy-3-methoxybenzyl alcohol (HMP) at 25 °C and a 24% yield to MMP at 50 °C suggesting a possibility to tune the products selectivity with the change of reaction temperature. The

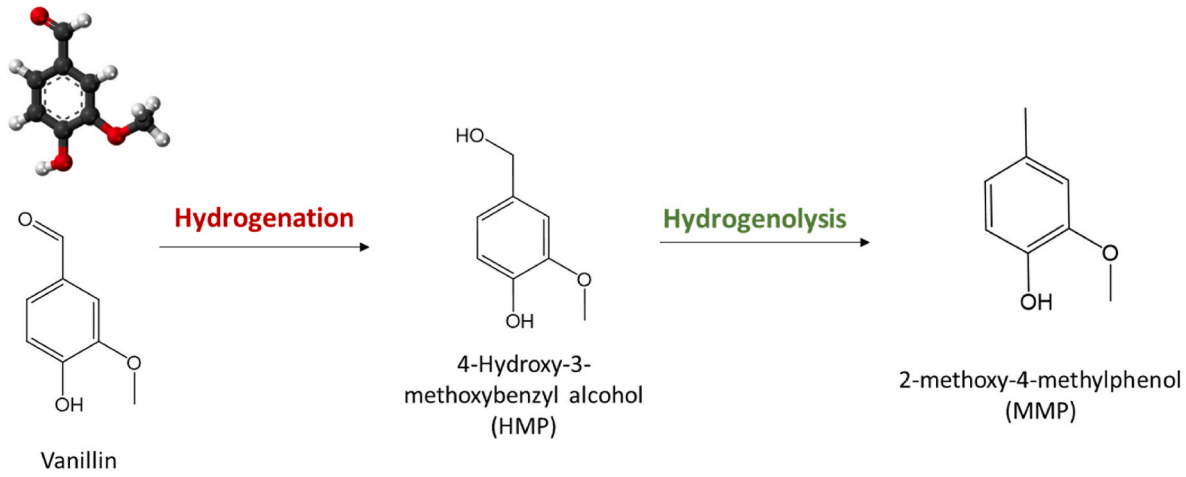

Scheme 10. Hydrogenation/hydrodeoxygenation of vanillin to MMP.

heterogenized complex resulted very easy to separate for recycling.

The Co@OMNC catalyst prepared for quinoline conversion, mentioned above, was also tested in vanillin hydrodeoxygenation [232]. The catalyst presented high yield and excellent selectivity to MMP (no by-products were observed) with a good control on Co-aggregation in acidic environment. As hydrogenation route the authors propose in first place HMP production (product suppressed in presence of FA) and subsequent hydrogenolysis to MMP [232]. Co@NC demonstrated to be versatile catalyst since a wide series of unsaturated hydrocarbons showed promising results, especially in the case of benzaldehyde and its derivatives. Zhou et al. [233] prepared using carboxymethyl cellulose (CMC) a Co nanocatalyst embedded in multi-layered N-doped graphene using urea as a non-corrosive activation agent (Co@NG). The urea generated porous belt-like nanostructure of high specific surface area and abundant nitrogen, thus providing multiple basic sites of high activity. For comparison purposes, carbon powder catalyst without nitrogen doping was also prepared, resulting in low vanillin conversion (<10%). On the contrary, a 57% of conversion with 100% selectivity to MMP was achieved over Co@NG catalyst attributed to the presence of higher surface area and strong basic sites. The Co was also used as dopant in Ni–P/HAP (hydroxyapatite) amorphous catalyst [234]. The incorporation of Co helped to suppress the formation of HMP and hence, promoted the production of MMP (up to 94%) with almost complete vanillin conversion (98%). The dispersion of metals improves for this Ni–Co–P amorphous alloy catalyst, resulting in stable particles against agglomeration and activity loss.

3.3.8. *Lignin*

Most of the model molecules described above originate from the lignin fraction of the LCB. Lignin is one of the three components of LCB which encompasses almost 30% of the existing organic carbon and is one of the major feedstocks of renewable aromatic compounds production. Unfortunately, it is mostly treated as a waste product or low value fuel since its combustion serves as energy supply in the pulp and paper industry [235].

Reductive catalytic fractionation (RCF) has emerged as a new biomass fractionation technology to obtain the maximum quantity of lignin-derived phenolic monomers (LDMPs). In the study of Park et al. [236], this technology is tested using different types of lignocellulosic biomass and Ni-based catalyst obtained via calcination of Ni–Al layered double hydroxides (Ni–Al LDHs) supported on activated carbon (AC) with aim to achieve (Ni@Al_2O_3/AC) with core-shell configuration. The used calcination method helped to obtain dispersed uniform and stable metal nanoparticles supported on high adsorption capacity carbons improving the overall catalytic activity. The presence of formic acid in this process has crucial and dual role: initially, acts as co-catalyst for lignin fractionation and subsequently, as hydrogen source to stabilize LDPMs via hydrodeoxygenation and hydrogenation. The versatility of the Ni@Al_2O_3/AC catalyst was tested over a series of lignocellulosic materials showing high degree of delignification >85%.

Oregui-Bengochea et al. [237] investigated lignin-to-liquids (LtL) methodology, using formic acid and ethanol as solvents over bimetallic NiMo catalyst supported on a sulphated Al_2O_3. They concluded that the solvent function is to help the stabilization of depolymerized monomers, ethanol being the most effective. Similarly, formic acid was found to act as H-donor and to assist the lignin fragmentation. Comparing experiments in batch mode or in semi-batch mode (feeding FA continuously), it was observed that FA decomposition reaction and reaction between lignin and formic acid are competing reactions and the depolymerization follows a formylation-deformylation-hydrogenolysis pathway. In a second study [238] of the same group, the mechanistic insights of LtL process were investigated deeper. After lignin depolymerization in smaller fragments, they must be hydrodeoxygenated to inhibit their re-polymerization (Scheme 11). Oil yield was determined by the first depolymerization reaction, being the HDO reaction conditions responsible for oil properties and compositions. Bimetallic NiMo catalyst is used in the process being the metallic Ni more active for depolymerization and Mo for HDO achieving significant activity.

The used catalytic systems and reaction conditions of different biomass derived molecules upgrade are summarized in Table 5.

4. Conclusion and future perspectives

Biomass upgrading reactions involving hydrogen are extremely important for the future sustainable development, especially pointing to biofuel or fuel additives production. The future of the biorefinery is conditioned by the efficient decrease of oxygen content in all bio-derived molecules and by the use of previously or *in-situ* generated green hydrogen. In this context the use of liquid organic hydrogen carrier, becomes an attractive possibility to generate and use hydrogen *in-situ* without being concerned on eventual H_2 gas transport or storage. An excellent liquid organic carriers to be used in bioreffinery reactions involving H_2 is formic acid due to its high volumetric hydrogen storage capacity and relatively low temperature of dehydrogenation and possibility to participate as H-donor in the catalytic hydrogen transfer reactions.

In general, the use of formic acid is not conditioned by the processes by themselves but by the price of the catalysts that must be used. Multifunctional catalysts are usually required to be able to dehydrogenate formic acid for *in situ* hydrogen production and to perform hydrogenation and/or hydrogenolysis of unsaturated and/or single bond.

Both, homogeneous and heterogeneous systems are designed for this

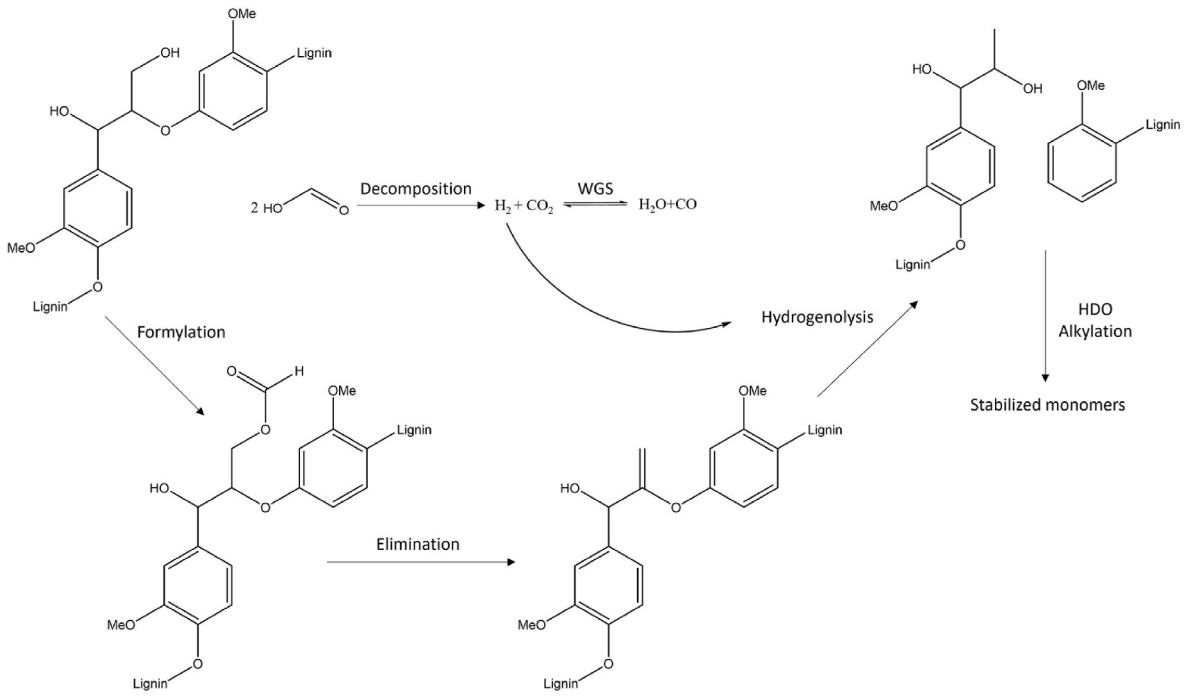

Scheme 11. Proposed process using formic acid to break down lignin through formylation, elimination, hydrogenolysis and subsequent monomer stabilization, adapted from Refs. [237,238] with permission from Wiley-VCH and Elsevier.

Table 5
Formic acid as hydrogen donor in the catalytic transfer hydrogenation of different biomass derived molecules.

Substrate[a]	Desired Product[b]	Solvent[c]	Catalysts	Conversion (%)	Yield[d] (%)	Time (h)	Temperature (°C)	Ref
BD	B	N_2	Pd/PS	100	99	3	250	[210]
GL	1,2-PDO	H_2O	Ni–Cu/Al_2O_3	90	82	24	220	[213]
GL	1,2-PDO	H_2O	Ni–Cu/Al_2O_3	43.9	83.4	10	220	[212]
GL	1,2-PDO	H_2O	Cu/ZrO_2	85	94	18	200	[214]
GL	1,2-PDO	H_2O	Cu:Zn:Al	73.8	53.9	1	250	[211]
P	CH	H_2O	Pd/AC	96	80	4	50	[217]
BnO	BnOH	H_2O/DMF	Ru/AlO(OH)	100	100	2	100	[219]
BnO	BnOH	H_2O	Ir@CN	99	99	18	100	[220]
BnO	BnOH	H_2O	Ir-bpy-CTF	86.0	–	12	40	[218]
BnO	BnOH	H_2O	Rh-bpy-CTF	95.4	–	12	40	[218]
Q	THQ	Et_3N/DMF	Au/TiO_2-R	99	96	10 min	130	[224]
Q	THQ	Et_3N/DMF	Au/NH_2-SBA-15	99	91	3	130	[225]
Q	THQ	i-PrOH	Co complex	>99	90	20	80	[226]
Q	THQ	H_2O	Co@OMNC-700	98.8	>99	4	140	[227]
V	MMP	H_2O	Au–Pt/CeO_2	99.9	99.8	4.5	150	[229]
V	MMP	H_2O	Co@NC-700	95.7	100	4	180	[232]
V	MMP	H_2O	Co@NG-6	98.5	99	6	160	[233]
V	MMP	i-PrOH	Ni–Co–P/HAP	97.86	93.97	5	200	[234]
V	MMP	H_2O	Pd/NMC	99	99	3	150	[230]
V	MMP	H_2O	Pd@HPC-DCD	100	100	12	80	[231]
V	MMP	H_2O/EA	Pd–Au/g-C_3N_4	99	99	1	RT	[178]
V	MMP	H_2O/KOH	IrPYA	100	24	5	50	[228]
V	VA	H_2O/KOH	IrPYA	100	70	1	25	[228]

[a] **BD**: 1,3-butadiene, **GL**: glycerol, **P**: phenol, **BnO**: benzaldehyde, **Q**: quinoline, **V**: vanillin.
[b] **B:** butene, **1,2-PDO**: 1,2-propanediol, **CH**: cyclohexanone, **BnOH**: benzyl alcohol, **THQ**: 1,2,3,4-tetrahydroquinoline, **MMP**: 2-methoxy-4-methylphenol, **VA**: vanillyl alcohol.
[c] **N_2**: nitrogen, **DMF**: dimethylformamide, **Et_3N**: Triethylamine, **i-PrOH**: isopropanol.
[d] Yield or Selectivity.

purpose. The homogeneous catalysts exhibited high efficiency, but a complicated and costly separation step and recyclability. On the contrary, heterogeneous catalysts are much more robust and easily recyclable. As for the nature of the active sites, noble and non-noble metal catalysts are widely explored in the upgrading of various biomass derived molecules. Although expensive the noble metals are preferred over the cheaper non-noble formulations requiring higher metal loading to achieve acceptable yields of desired product and suffering sometimes severe leaching problems. It appears that the future belongs to the bimetallic systems able to combine synergically two metals (noble-noble, non-noble-non-noble or noble-non-noble) in a manner to control activity rate to achieve high conversion and selectivity toward desired products at low consummative cost.

The role of the supports' nature in the heterogeneous systems is also

very important; they are not only spectators. Supports, such as functionalized carbons and metal oxides could provide surface oxygen vacancies (functional groups) interacting directly with the oxygen containing functional groups of the biomass molecule and available basic sites that capture directly hydrogen from formic acid, thus facilitating the H donation. Supports like carbon nitride becomes more and more interesting providing the possibility to modify the electronic properties of the dispersed metal via different metal-support interactions. Moreover, the textural properties of the support (surface area, porosity, hydrophilicity … etc.) also play an essential role in catalyst stabilization.

Obviously the choice of reaction conditions (temperature, initial concentration, time, solvent nature and amount … etc.) and chemical reactors is another key step when envisaging formic acid use as hydrogen generating agent. In many cases, the use of formic acid instead of molecular hydrogen leads to improved selectivity in CTH/HDO mediated biomass upgrading reactions but still the selectivity and product yield control in some reactions should be well optimized.

The operational and safety drawbacks of H_2 transportation, storage, and use along with its high cost, positions the use of liquid hydrogen carriers as an excellent approach to potentiate the use of in-situ generated hydrogen in biorefinery. Among the liquid organic carriers, formic acid needs special attention of being easily producible from biomass. The possibility to use formic acid produced after oxidation of glucose or as a co-product of the levulinic acid allows the decrease of the investment requirement to cost the catalytic systems. So, any future work must be dedicated to propose a stable catalyst formulation at low price able to work in all hydrogen involved biorefinery reactions. In the last decade, the catalytic society has advanced with giant steps toward the development of such systems and the time to increase the industrial production and use of formic acid will come sooner than expected.

Declaration of competing interest

The authors declare that they have no known competing financial interests or personal relationships that could have appeared to influence the work reported in this paper.

Acknowledgements

Financial support was obtained from Spanish Ministerio de Ciencia e Innovación (MCIN/AEI/10.13039/501100011033/) and for FEDER Funds una manera de hacer Europa), Project PID2020-113809RB-C32. Also the financial support from Junta de Andalucía via Consejería de Transformación Económica, Industria, Conocimiento y Universidades and its PAIDI 2020 program (Grant P18-RT-3405) co-financed by FEDER funds from the European Union is highly appreciated.

References

[1] L.T. Mika, E. Cséfalvay, Á. Németh, Catalytic conversion of carbohydrates to initial platform chemicals: chemistry and sustainability, Chem. Rev. 118 (2018) 505–613, https://doi.org/10.1021/ACS.CHEMREV.7B00395/ASSET/IMAGES/MEDIUM/CR-2017-00395A_0017. GIF.

[2] S. Chu, A. Majumdar, Opportunities and challenges for a sustainable energy future, Nature 488 (2012) 7411, https://doi.org/10.1038/nature11475, 488 (2012) 294–303.

[3] N.S. Lewis, D.G. Nocera, Powering the planet: chemical challenges in solar energy utilization, Proc. Natl. Acad. Sci. U. S. A. 103 (2006) 15729–15735, https://doi.org/10.1073/PNAS.0603395103/ASSET/3DE8043E-D8A1-44B0-AFD0-FD0C4CC001CE/ASSETS/GRAPHIC/ZPQ03906360600E4. JPEG.

[4] I. Valdez-Vazquez, J.A. Acevedo-Benítez, C. Hernández-Santiago, Distribution and potential of bioenergy resources from agricultural activities in Mexico, Renew. Sustain. Energy Rev. 14 (2010) 2147–2153, https://doi.org/10.1016/J.RSER.2010.03.034.

[5] X. Wu, N. Luo, S. Xie, H. Zhang, Q. Zhang, F. Wang, Y. Wang, Photocatalytic transformations of lignocellulosic biomass into chemicals, Chem. Soc. Rev. 49 (2020) 6198–6223, https://doi.org/10.1039/D0CS00314J.

[6] A. Lorenci Woiciechowski, C.J. Dalmas Neto, L. Porto de Souza Vandenberghe, D. P. de Carvalho Neto, A.C. Novak Sydney, L.A.J. Letti, S.G. Karp, L.A. Zevallos Torres, C.R. Soccol, Lignocellulosic biomass: acid and alkaline pretreatments and their effects on biomass recalcitrance – conventional processing and recent advances, Bioresour. Technol. 304 (2020), 122848, https://doi.org/10.1016/J.BIORTECH.2020.122848.

[7] A.R. Ardiyanti, S.A. Khromova, R.H. Venderbosch, V.A. Yakovlev, H.J. Heeres, Catalytic hydrotreatment of fast-pyrolysis oil using non-sulfided bimetallic Ni-Cu catalysts on a δ-Al2O3 support, Appl. Catal., B 117–118 (2012) 105–117, https://doi.org/10.1016/J.APCATB.2011.12.032.

[8] M.J. Gilkey, B. Xu, Heterogeneous catalytic transfer hydrogenation as an effective pathway in biomass upgrading, ACS Catal. 6 (2016) 1420–1436, https://doi.org/10.1021/ACSCATAL.5B02171/ASSET/IMAGES/LARGE/CS-2015-02171M_0018. JPEG.

[9] N. Arun, R.V. Sharma, A.K. Dalai, Green diesel synthesis by hydrodeoxygenation of bio-based feedstocks: strategies for catalyst design and development, Renew. Sustain. Energy Rev. 48 (2015) 240–255, https://doi.org/10.1016/J.RSER.2015.03.074.

[10] P. Puthiaraj, K. Kim, W. Ahn, Highlights of the Present Work Graphical Abstract SC, Catal Today, 2018.

[11] P. Xiao, J. Zhu, D. Zhao, Z. Zhao, F. Zaera, Y. Zhu, Porous LaFeO 3 prepared by an in situ carbon templating method for catalytic transfer hydrogenation reactions, ACS Appl. Mater. Interfaces 11 (2019) 15517–15527, https://doi.org/10.1021/ACSAMI.9B00506/ASSET/IMAGES/MEDIUM/AM-2019-005069_M003. GIF.

[12] R.A.W. Johnstone, A.H. Wilby, I.D. Entwistle, Heterogeneous catalytic transfer hydrogenation and its relation to other methods for reduction of organic compounds, Chem. Rev. 85 (1985) 129–170, https://doi.org/10.1021/CR00066A003/ASSET/CR00066A003.FP.PNG_V03.

[13] J. Yuan, S.S. Li, L. Yu, Y.M. Liu, Y. Cao, H.Y. He, K.N. Fan, Copper-based catalysts for the efficient conversion of carbohydrate biomass into γ-valerolactone in the absence of externally added hydrogen, Energy Environ. Sci. 6 (2013) 3308–3313, https://doi.org/10.1039/C3EE40857D.

[14] L. Deng, J. Li, D.-M. Lai, Y. Fu, Q.-X. Guo, L. Deng, J. Li, D. Lai, Y. Fu, Q. Guo, Catalytic conversion of biomass-derived carbohydrates into γ-valerolactone without using an external H2 supply, Angew. Chem. 121 (2009) 6651–6654, https://doi.org/10.1002/ANGE.200902281.

[15] A. Demirbaş, Biomass resource facilities and biomass conversion processing for fuels and chemicals, Energy Convers. Manag. 42 (2001) 1357–1378, https://doi.org/10.1016/S0196-8904(00)00137-0.

[16] T. Wang, J. Du, Y. Sun, X. Tang, Z.J. Wei, X. Zeng, S.J. Liu, L. Lin, Catalytic transfer hydrogenation of biomass-derived furfural to furfuryl alcohol with formic acid as hydrogen donor over CuCs-MCM catalyst, Chin. Chem. Lett. 32 (2021) 1186–1190, https://doi.org/10.1016/J.CCLET.2020.07.044.

[17] D.A. Bulushev, J.R.H. Ross, Towards sustainable production of formic acid, ChemSusChem 11 (2018) 821–836, https://doi.org/10.1002/CSSC.201702075.

[18] S. Enthaler, J. Von Langermann, T. Schmidt, Carbon dioxide and formic acid—the couple for environmental-friendly hydrogen storage? Energy Environ. Sci. 3 (2010) 1207–1217, https://doi.org/10.1039/B907569K.

[19] W. Yang, P. Li, D. Bo, H. Chang, The optimization of formic acid hydrolysis of xylose in furfural production, Carbohydr. Res. 357 (2012) 53–61, https://doi.org/10.1016/J.CARRES.2012.05.020.

[20] M. Navlani-García, K. Mori, D. Salinas-Torres, Y. Kuwahara, H. Yamashita, New approaches toward the hydrogen production from formic acid dehydrogenation over pd-based heterogeneous catalysts, Front Mater 6 (2019) 44, https://doi.org/10.3389/FMATS.2019.00044/BIBTEX.

[21] X. Chen, Y. Liu, J. Wu, Sustainable production of formic acid from biomass and carbon dioxide, Mol. Catal. 483 (2020), 110716, https://doi.org/10.1016/J.MCAT.2019.110716.

[22] J.T. Overpeck, C. Conde, A call to climate action, Science 364 (2019) (1979) 807, https://doi.org/10.1126/SCIENCE.AAY1525/ASSET/CDFA2890-DA76-4B7E-B3A4-98A5C44498B3/ASSETS/GRAPHIC/364_807_F2. JPEG.

[23] D.A. Bulushev, L.G. Bulusheva, Https://Doi.Org/10.1080/01614940.2020.1864860, Catalysts with Single Metal Atoms for the Hydrogen Production from Formic Acid, vol. 64, 2021, pp. 835–874, https://doi.org/10.1080/01614940.2020.1864860.

[24] M. Mikkelsen, M. Jørgensen, F.C. Krebs, The teraton challenge. A review of fixation and transformation of carbon dioxide, Energy Environ. Sci. 3 (2010) 43–81, https://doi.org/10.1039/B912904A.

[25] J. Duan, Z. Xiang, H. Zhang, B. Zhang, X. Xiang, Pd-Co2P nanoparticles supported on N-doped biomass-based carbon microsheet with excellent catalytic performance for hydrogen evolution from formic acid, Appl. Surf. Sci. 530 (2020), 147191, https://doi.org/10.1016/J.APSUSC.2020.147191.

[26] O. Sneka-Płatek, K. Kaźmierczak, M. Jędrzejczyk, P. Sautet, N. Keller, C. Michel, A.M. Ruppert, Understanding the influence of the composition of the AgPd catalysts on the selective formic acid decomposition and subsequent levulinic acid hydrogenation, Int. J. Hydrogen Energy 45 (2020) 17339–17353, https://doi.org/10.1016/J.IJHYDENE.2020.04.180.

[27] A.M. Ruppert, M. Jędrzejczyk, N. Potrzebowska, K. Kaźmierczak, M. Brzezińska, O. Sneka-Płatek, P. Sautet, N. Keller, C. Michel, J. Grams, Supported gold–nickel nano-alloy as a highly efficient catalyst in levulinic acid hydrogenation with formic acid as an internal hydrogen source, Catal. Sci. Technol. 8 (2018) 4318–4331, https://doi.org/10.1039/C8CY00462E.

[28] J.S. Yoo, F. Abild-Pedersen, J.K. Nørskov, F. Studt, Theoretical analysis of transition-metal catalysts for formic acid decomposition, ACS Catal. 4 (2014) 1226–1233, https://doi.org/10.1021/cs400664z.

[29] S. Schlussel, S. Kwon, A review of formic acid decomposition routes on transition metals for its potential use as a liquid H2 carrier, Kor. J. Chem. Eng. 39 (2022) 2883–2895, https://doi.org/10.1007/s11814-022-1276-z.

[30] K. Jiang, K. Xu, S. Zou, W. Bin Cai, B-doped pd catalyst: boosting room-temperature hydrogen production from formic acid-formate solutions, J. Am. Chem. Soc. 136 (2014) 4861–4864, https://doi.org/10.1021/JA5008917.
[31] K. Sordakis, C. Tang, L.K. Vogt, H. Junge, P.J. Dyson, M. Beller, G. Laurenczy, Homogeneous catalysis for sustainable hydrogen storage in formic acid and alcohols, Chem. Rev. 118 (2018) 372–433, https://doi.org/10.1021/acs.chemrev.7b00182.
[32] M. Onishi, Decomposition of formic acid catalyzed by hydrido (phosphonite) cobalt (I) under photoirradiation, J. Mol. Catal. 80 (1993) 145–149, https://doi.org/10.1016/0304-5102(93)85073-3.
[33] A. Boddien, B. Loges, F. Gärtner, C. Torborg, K. Fumino, H. Junge, R. Ludwig, M. Beller, Iron-catalyzed hydrogen production from formic acid, J. Am. Chem. Soc. 132 (2010) 8924–8934, https://doi.org/10.1021/JA100925N/SUPPL_FILE/JA100925N_SI_001.PDF.
[34] A.M. Tondreau, J.M. Boncella, 1,2-Addition of formic or oxalic acid to -N{CH2CH2(PiPr2)}2-supported Mn(I) dicarbonyl complexes and the manganese-mediated decomposition of formic acid, Organometallics 35 (2016) 2049–2052, https://doi.org/10.1021/ACS.ORGANOMET.6B00274/SUPPL_FILE/OM6B00274_SI_002.CIF.
[35] S. Enthaler, A. Brück, A. Kammer, H. Junge, E. Irran, S. Gülak, Exploring the reactivity of nickel pincer complexes in the decomposition of formic acid to CO2/H2 and the hydrogenation of NaHCO3 to HCOONa, ChemCatChem 7 (2015) 65–69, https://doi.org/10.1002/CCTC.201402716.
[36] M.C. Neary, G. Parkin, Nickel-catalyzed release of H2 from formic acid and a new method for the synthesis of zerovalent Ni(PMe3)4, Dalton Trans. 45 (2016) 14645–14650, https://doi.org/10.1039/C6DT01499B.
[37] T. Nakajima, Y. Kamiryo, M. Kishimoto, K. Imai, K. Nakamae, Y. Ura, T. Tanase, Synergistic Cu2 catalysts for formic acid dehydrogenation, J. Am. Chem. Soc. 141 (2019) 8732–8736, https://doi.org/10.1021/JACS.9B03532/SUPPL_FILE/JA9B03532_SI_002.CIF.
[38] N. Scotti, R. Psaro, N. Ravasio, F. Zaccheria, A new Cu-based system for formic acid dehydrogenation, RSC Adv. 4 (2014) 61514–61517, https://doi.org/10.1039/C4RA11031E.
[39] W. Gan, P.J. Dyson, G. Laurenczy, Hydrogen storage and delivery: immobilization of a highly active homogeneous catalyst for the decomposition of formic acid to hydrogen and carbon dioxide, React. Kinet. Catal. Lett. 98 (2009) 205–213, https://doi.org/10.1007/S11144-009-0096-Z.
[40] P.J.C. Hausoul, C. Broicher, R. Vegliante, C. Göb, R. Palkovits, Solid molecular phosphine catalysts for formic acid decomposition in the biorefinery, Angew Chem. Int. Ed. Engl. 55 (2016) 5597–5601, https://doi.org/10.1002/ANIE.201510681.
[41] I. Yuranov, N. Autissier, K. Sordakis, A.F. Dalebrook, M. Grasemann, V. Orava, P. Cendula, L. Gubler, G. Laurenczy, Heterogeneous catalytic reactor for hydrogen production from formic acid and its use in polymer electrolyte fuel cells, ACS Sustain. Chem. Eng. 6 (2018) 6635–6643, https://doi.org/10.1021/ACSSUSCHEMENG.8B00423.
[42] G.H. Gunasekar, H. Kim, S. Yoon, Dehydrogenation of formic acid using molecular Rh and Ir catalysts immobilized on bipyridine-based covalent triazine frameworks, Sustain. Energy Fuels 3 (2019) 1042–1047, https://doi.org/10.1039/C9SE00002J.
[43] A.V. Bavykina, M.G. Goesten, F. Kapteijn, M. Makkee, J. Gascon, Efficient production of hydrogen from formic acid using a covalent triazine framework supported molecular catalyst, ChemSusChem 8 (2015) 809–812, https://doi.org/10.1002/CSSC.201403173.
[44] C. Shen, K. Dong, Z. Wei, X. Tian, In Silico Investigation of Ligand-Regulated Palladium-Catalysed Formic Acid Dehydrative Decomposition under Acidic Conditions, 2021, https://doi.org/10.26434/CHEMRXIV-2021-DD56W-V3.
[45] M. Iglesias, F.J. Fernández-Alvarez, Advances in nonprecious metal homogeneously catalyzed formic acid dehydrogenation, Catalysts 11 (2021) 1288, https://doi.org/10.3390/CATAL11111288, 11 (2021) 1288.
[46] F.Z. Song, Q.L. Zhu, N. Tsumori, Q. Xu, Diamine-alkalized reduced graphene oxide: immobilization of sub-2 nm palladium nanoparticles and optimization of catalytic activity for dehydrogenation of formic acid, ACS Catal. 5 (2015) 5141–5144, https://doi.org/10.1021/ACSCATAL.5B01411/ASSET/IMAGES/LARGE/CS-2015-01411K_0004. JPEG.
[47] C. Hu, J.K. Pulleri, S.W. Ting, K.Y. Chan, Activity of Pd/C for hydrogen generation in aqueous formic acid solution, Int. J. Hydrogen Energy 39 (2014) 381–390, https://doi.org/10.1016/J.IJHYDENE.2013.10.067.
[48] J.L. Santos, C. Megías-Sayago, S. Ivanova, M.Á. Centeno, J.A. Odriozola, Functionalized biochars as supports for Pd/C catalysts for efficient hydrogen production from formic acid, Appl. Catal., B 282 (2021), 119615, https://doi.org/10.1016/J.APCATB.2020.119615.
[49] J.L. Santos, C. Megías-Sayago, S. Ivanova, M.Á. Centeno, J.A. Odriozola, Structure-sensitivity of formic acid dehydrogenation reaction over additive-free Pd NPs supported on activated carbon, Chem. Eng. J. 420 (2021), 127641, https://doi.org/10.1016/J.CEJ.2020.127641.
[50] Q.Y. Bi, X.L. Du, Y.M. Liu, Y. Cao, H.Y. He, K.N. Fan, Efficient subnanometric gold-catalyzed hydrogen generation via formic acid decomposition under ambient conditions, J. Am. Chem. Soc. 134 (2012) 8926–8933, https://doi.org/10.1021/JA301696E/SUPPL_FILE/JA301696E_SI_001.PDF.
[51] Q.Y. Bi, J.D. Lin, Y.M. Liu, H.Y. He, F.Q. Huang, Y. Cao, Gold supported on zirconia polymorphs for hydrogen generation from formic acid in base-free aqueous medium, J. Power Sources 328 (2016) 463–471, https://doi.org/10.1016/J.JPOWSOUR.2016.08.056.
[52] A.M. Ruppert, M. Jędrzejczyk, O. Sneka-Płatek, N. Keller, A.S. Dumon, C. Michel, P. Sautet, J. Grams, Ru catalysts for levulinic acid hydrogenation with formic acid as a hydrogen source, Green Chem. 18 (2016) 2014–2028, https://doi.org/10.1039/C5GC02200B.
[53] J.L. Santos, C. León, G. Monnier, S. Ivanova, M.Á. Centeno, J.A. Odriozola, Bimetallic PdAu catalysts for formic acid dehydrogenation, Int. J. Hydrogen Energy 45 (2020) 23056–23068, https://doi.org/10.1016/J.IJHYDENE.2020.06.076.
[54] T. Feng, J.M. Wang, S.T. Gao, C. Feng, N.Z. Shang, C. Wang, X.L. Li, Covalent triazine frameworks supported CoPd nanoparticles for boosting hydrogen generation from formic acid, Appl. Surf. Sci. 469 (2019) 431–436, https://doi.org/10.1016/J.APSUSC.2018.11.036.
[55] Y. Hou, M. Niu, W. Wu, Catalytic oxidation of biomass to formic acid using O2as an oxidant, Ind. Eng. Chem. Res. 59 (2020) 16899–16910, https://doi.org/10.1021/ACS.IECR.0C01088/ASSET/IMAGES/LARGE/IE0C01088_0006. JPEG.
[56] J. Hietala, A. Vuori, P. Johnsson, I. Pollari, W. Reutemann, H. Kieczka, Formic Acid, Ullmann's Encyclopedia of Industrial Chemistry, 2016, pp. 1–22, https://doi.org/10.1002/14356007.A12_013.PUB3.
[57] P. Sarkar, S. Riyajuddin, A. Das, A. Hazra Chowdhury, K. Ghosh, S.M. Islam, Mesoporous covalent organic framework: an active photo-catalyst for formic acid synthesis through carbon dioxide reduction under visible light, Mol. Catal. 484 (2020), 110730, https://doi.org/10.1016/J.MCAT.2019.110730.
[58] X. Wei, Y. Li, L. Chen, J. Shi, Formic acid electro-synthesis by concurrent cathodic CO2 reduction and anodic CH3OH oxidation, Angew. Chem. Int. Ed. 60 (2021) 3148–3155, https://doi.org/10.1002/ANIE.202012066.
[59] Y. Lee, Y. Yu, H. Tanaya Das, J. Theerthagiri, S. Jun Lee, A. Min, G.A. Kim, H. C. Choi, M.Y. Choi, Pulsed laser-driven green synthesis of trimetallic AuPtCu nanoalloys for formic acid electro-oxidation in acidic environment, Fuel 332 (2023), 126164, https://doi.org/10.1016/J.FUEL.2022.126164.
[60] S. Chatterjee, I. Dutta, Y. Lum, Z. Lai, K.W. Huang, Enabling storage and utilization of low-carbon electricity: power to formic acid, Energy Environ. Sci. 14 (2021) 1194–1246, https://doi.org/10.1039/D0EE03011B.
[61] P.K. Sahoo, T. Zhang, S. Das, Oxidative transformation of biomass into formic acid, Eur. J. Org Chem. 2021 (2021) 1331–1343, https://doi.org/10.1002/EJOC.202001514.
[62] J. Dai, L. Peng, H. Li, Intensified ethyl levulinate production from cellulose using a combination of low loading H2SO4 and Al(OTf)3, Catal. Commun. 103 (2018) 116–119, https://doi.org/10.1016/J.CATCOM.2017.10.007.
[63] K. Kong, D. Li, W. Ma, Q. Zhou, G. Tang, Z. Hou, Aluminum(III) triflate-catalyzed selective oxidation of glycerol to formic acid with hydrogen peroxide, Chin. J. Catal. 40 (2019) 534–542, https://doi.org/10.1016/S1872-2067(19)63319-X.
[64] A. Takagaki, W. Obata, T. Ishihara, Oxidative conversion of glucose to formic acid as a renewable hydrogen source using an abundant solid base catalyst, ChemistryOpen 10 (2021) 954–959, https://doi.org/10.1002/OPEN.202100074.
[65] L. Wu, Y. Yang, J. Cheng, X. Shi, H. Zhong, F. Jin, Highly efficient conversion of carbohydrates into formic acid with a heterogeneous MgO catalyst at near-ambient temperatures, ACS Sustain. Chem. Eng. 10 (2022) 15423–15436, https://doi.org/10.1021/ACSSUSCHEMENG.2C04502/ASSET/IMAGES/LARGE/SC2C04502_0011. JPEG.
[66] H.A. Kılıç, E. Kılıç, L. Erden, Y. Gök, Highly selective oxidation of glucose to formic acid over synthesized hydrotalcite-like catalysts under base free mild conditions, Res. Chem. Intermed. 48 (2022) 4079–4103, https://doi.org/10.1007/S11164-022-04811-9/FIGURES/20.
[67] H.A. Kılıç, Y. Gök, Selective glucose oxidation to organic acids over synthesized bimetallic oxides at low temperatures, React. Kinet. Mech. Catal. 136 (2023) 267–286, https://doi.org/10.1007/S11144-022-02342-3/FIGURES/9.
[68] M. Yuan, D. Li, X. Zhao, W. Ma, K. Kong, W. Ni, Q. Gu, Z. Hou, Selective oxidation of glycerol with hydrogen peroxide using silica-encapsulated heteropolyacid catalyst, Wuli Huaxue Xuebao/Acta Phys. - Chim. Sin. 34 (2018) 886–895, https://doi.org/10.3866/PKU.WHXB201711151.
[69] J. Albert, Selective oxidation of lignocellulosic biomass to formic acid and high-grade cellulose using tailor-made polyoxometalate catalysts, Faraday Discuss 202 (2017) 99–109, https://doi.org/10.1039/C7FD00047B.
[70] J. Reichert, J. Albert, Detailed kinetic investigations on the selective oxidation of biomass to formic acid (OxFA process) using model substrates and real biomass, ACS Sustain. Chem. Eng. 5 (2017) 7383–7392, https://doi.org/10.1021/ACSSUSCHEMENG.7B01723/ASSET/IMAGES/LARGE/SC-2017-01723K_0006. JPEG.
[71] S. Maerten, C. Kumpidet, D. Voß, A. Bukowski, P. Wasserscheid, J. Albert, Glucose oxidation to formic acid and methyl formate in perfect selectivity, Green Chem. 22 (2020) 4311–4320, https://doi.org/10.1039/D0GC01169J.
[72] T. Lu, Y. Hou, W. Wu, M. Niu, S. Ren, Z. Lin, V.K. Ramani, Catalytic oxidation of biomass to oxygenated chemicals with exceptionally high yields using H5PV2Mo10O40, Fuel 216 (2018) 572–578, https://doi.org/10.1016/J.FUEL.2017.12.044.
[73] J. Albert, M. Mendt, M. Mozer, D. Voß, Explaining the role of vanadium in homogeneous glucose transformation reactions using NMR and EPR spectroscopy, Appl. Catal. Gen. 570 (2019) 262–270, https://doi.org/10.1016/J.APCATA.2018.10.030.
[74] D. Voß, R. Dietrich, M. Stuckart, J. Albert, Switchable catalytic polyoxometalate-based systems for biomass conversion to carboxylic acids, ACS Omega 5 (2020) 19082–19091, https://doi.org/10.1021/ACSOMEGA.0C02430/ASSET/IMAGES/MEDIUM/AO0C02430_M002. GIF.
[75] Y. Hou, Z. Lin, M. Niu, S. Ren, W. Wu, Conversion of cellulose into formic acid by iron(III)-Catalyzed oxidation with O2 in acidic aqueous solutions, ACS Omega 3 (2018) 14910–14917, https://doi.org/10.1021/ACSOMEGA.8B01409/ASSET/IMAGES/LARGE/AO-2018-01409X_0007. JPEG.

[76] J. Li, R.L. Smith, S. Xu, D. Li, J. Yang, K. Zhang, F. Shen, Manganese oxide as an alternative to vanadium-based catalysts for effective conversion of glucose to formic acid in water, Green Chem. 24 (2022) 315–324, https://doi.org/10.1039/D1GC03637H.
[77] S. Xu, J. Yang, J. Li, F. Shen, Highly efficient oxidation of biomass xylose to formic acid with CeOx-promoted MnOx catalyst in water, ACS Sustain. Chem. Eng. 11 (2023) 921–930, https://doi.org/10.1021/ACSSUSCHEMENG.2C04940/ASSET/IMAGES/LARGE/SC2C04940_0009. JPEG.
[78] H. Guo, J. Li, S. Xu, J. Yang, G.H. Chong, F. Shen, Mo-modified MnOx for the efficient oxidation of high-concentration glucose to formic acid in water, Fuel Process. Technol. 242 (2023), 107662, https://doi.org/10.1016/J.FUPROC.2023.107662.
[79] D. Di Menno Di Bucchianico, Y. Wang, J.C. Buvat, Y. Pan, V. Casson Moreno, S. Leveneur, Production of levulinic acid and alkyl levulinates: a process insight, Green Chem. 24 (2022) 614–646, https://doi.org/10.1039/D1GC02457D.
[80] D.W. Rackemann, W.O. Doherty, The conversion of lignocellulosics to levulinic acid, Biofuels, Bioproducts and Biorefining 5 (2011) 198–214, https://doi.org/10.1002/BBB.267.
[81] A. Morone, M. Apte, R.A. Pandey, Levulinic acid production from renewable waste resources: bottlenecks, potential remedies, advancements and applications, Renew. Sustain. Energy Rev. 51 (2015) 548–565, https://doi.org/10.1016/J.RSER.2015.06.032.
[82] T. Werpy, G. Petersen, Top value added chemicals from biomass: volume I – results of screening for potential candidates from sugars and synthesis gas, Us Nrel, Medium: ED; Size, 2004, p. 76, https://doi.org/10.2172/15008859.
[83] T. Boonyakarn, P. Wataniyakul, P. Boonnoun, A.T. Quitain, T. Kida, M. Sasaki, N. Laosiripojana, B. Jongsomjit, A. Shotipruk, Enhanced levulinic acid production from cellulose by combined brønsted hydrothermal carbon and Lewis acid catalysts, Ind. Eng. Chem. Res. 58 (2019) 2697–2703, https://doi.org/10.1021/ACS.IECR.8B05332/ASSET/IMAGES/LARGE/IE-2018-053329_0005. JPEG.
[84] F. Yu, R. Zhong, H. Chong, M. Smet, W. Dehaen, B.F. Sels, Fast catalytic conversion of recalcitrant cellulose into alkyl levulinates and levulinic acid in the presence of soluble and recoverable sulfonated hyperbranched poly(arylene oxindole)s, Green Chem. 19 (2017) 153–163, https://doi.org/10.1039/C6GC02130A.
[85] B. Girisuta, L.P.B.M. Janssen, H.J. Heeres, A kinetic study on the decomposition of 5-hydroxymethylfurfural into levulinic acid, Green Chem. 8 (2006) 701–709, https://doi.org/10.1039/B518176C.
[86] D.M. Alonso, S.G. Wettstein, M.A. Mellmer, E.I. Gurbuz, J.A. Dumesic, Integrated conversion of hemicellulose and cellulose from lignocellulosic biomass, Energy Environ. Sci. 6 (2012) 76–80, https://doi.org/10.1039/C2EE23617F.
[87] H.J. Feng, X.C. Li, H. Qian, Y.F. Zhang, D.H. Zhang, D. Zhao, S.G. Hong, N. Zhang, Efficient and sustainable hydrogenation of levulinic-acid to gamma-valerolactone in aqueous solution over acid-resistant CePO4/Co2P catalysts, Green Chem. 21 (2019) 1743–1756, https://doi.org/10.1039/C9GC00482C.
[88] A.M.R. Galletti, C. Antonetti, V. De Luise, M. Martinelli, A sustainable process for the production of γ-valerolactone by hydrogenation of biomass-derived levulinic acid, Green Chem. 14 (2012) 688–694, https://doi.org/10.1039/C2GC15872H.
[89] G. Novodárszki, H.E. Solt, J. Valyon, F. Lónyi, J. Hancsók, D. Deka, R. Tuba, M. R. Mihályi, Selective hydroconversion of levulinic acid to γ-valerolactone or 2-methyltetrahydrofuran over silica-supported cobalt catalysts, Catal. Sci. Technol. 9 (2019) 2291–2304, https://doi.org/10.1039/C9CY00168A.
[90] J. Cui, J. Tan, Y. Zhu, F. Cheng, Aqueous hydrogenation of levulinic acid to 1,4-pentanediol over Mo-modified Ru/activated carbon catalyst, ChemSusChem 11 (2018) 1316–1320, https://doi.org/10.1002/CSSC.201800038.
[91] P. Sun, G. Gao, Z. Zhao, C. Xia, F. Li, Stabilization of cobalt catalysts by embedment for efficient production of valeric biofuel, ACS Catal. 4 (2014) 4136–4142, https://doi.org/10.1021/CS501409S/SUPPL_FILE/CS501409S_SI_001.PDF.
[92] L. Wu, S. Dutta, M. Mascal, Efficient, chemical-catalytic approach to the production of 3-hydroxypropanoic acid by oxidation of biomass-derived levulinic acid with hydrogen peroxide, ChemSusChem 8 (2015) 1167–1169, https://doi.org/10.1002/CSSC.201500025.
[93] D. Carnevali, M.G. Rigamonti, T. Tabanelli, G.S. Patience, F. Cavani, Levulinic acid upgrade to succinic acid with hydrogen peroxide, Appl. Catal. Gen. 563 (2018) 98–104, https://doi.org/10.1016/J.APCATA.2018.06.034.
[94] A.S. Amarasekara, T.B. Singh, E. Larkin, M.A. Hasan, H.J. Fan, NaOH catalyzed condensation reactions between levulinic acid and biomass derived furan-aldehydes in water, Ind. Prod. 65 (2015) 546–549, https://doi.org/10.1016/J.INDCROP.2014.10.005.
[95] S. Van De Vyver, S. Helsen, J. Geboers, F. Yu, J. Thomas, M. Smet, W. Dehaen, Y. Román-Leshkov, I. Hermans, B.F. Sels, Mechanistic insights into the kinetic and regiochemical control of the thiol-promoted catalytic synthesis of diphenolic acid, ACS Catal. 2 (2012) 2700–2704, https://doi.org/10.1021/CS300635R/SUPPL_FILE/CS300635R_SI_001.PDF.
[96] I.T. Horváth, H. Mehdi, V. Fábos, L. Boda, L.T. Mika, γ-Valerolactone—a sustainable liquid for energy and carbon-based chemicals, Green Chem. 10 (2008) 238–242, https://doi.org/10.1039/B712863K.
[97] L. Qi, I.T. Horváth, Catalytic conversion of fructose to γ-valerolactone in γ-valerolactone, ACS Catal. 2 (2012) 2247–2249, https://doi.org/10.1021/CS300428F/SUPPL_FILE/CS300428F_SI_001.PDF.
[98] D.R. Dodds, R.A. Gross, Chemistry: chemicals from biomass, Science 318 (2007) (1979) 1250–1251, https://doi.org/10.1126/SCIENCE.1146356/ASSET/962A5427-636B-4714-9BFC-10F74AE14A44/ASSETS/GRAPHIC/1250-1. GIF.
[99] J.Q. Bond, D. Martin Alonso, R.M. West, J.A. Dumesic, γ-valerolactone ring-opening and decarboxylation over SiO 2/Al2O3 in the presence of water, Langmuir 26 (2010) 16291–16298, https://doi.org/10.1021/LA101424A/ASSET/IMAGES/LARGE/LA-2010-01424A_0007. JPEG.
[100] D.M. Alonso, S.G. Wettstein, J.A. Dumesic, Gamma-valerolactone , a sustainable platform molecule derived from lignocellulosic biomass, Green Chem. 15 (2013) 584–595, https://doi.org/10.1039/C3GC37065H.
[101] S. Choi, C.W. Song, J.H. Shin, S.Y. Lee, Biorefineries for the production of top building block chemicals and their derivatives, Metab. Eng. 28 (2015) 223–239, https://doi.org/10.1016/J.YMBEN.2014.12.007.
[102] A.M. Hengne, B.S. Kadu, N.S. Biradar, R.C. Chikate, C.V. Rode, Transfer hydrogenation of biomass-derived levulinic acid to γ-valerolactone over supported Ni catalysts, RSC Adv. 6 (2016) 59753–59761, https://doi.org/10.1039/C6RA08637C.
[103] C. Li, G. Xu, Y. Zhai, X. Liu, Y. Ma, Y. Zhang, Hydrogenation of biomass-derived ethyl levulinate into γ-valerolactone by activated carbon supported bimetallic Ni and Fe catalysts, Fuel 203 (2017) 23–31, https://doi.org/10.1016/J.FUEL.2017.04.082.
[104] C.E. Bounoukta, C. Megías-Sayago, J.C. Navarro, F. Ammari, S. Ivanova, M.Á. Centeno, J.A. Odriozola, Functionalized biochars as supports for Ru/C catalysts: tunable and efficient materials for γ-valerolactone production, Nanomaterials 13 (2023) 1129, https://doi.org/10.3390/NANO13061129/S1.
[105] C.E. Bounoukta, C. Megías-Sayago, N. Rendón, F. Ammari, A. Penkova, S. Ivanova, M.Á. Centeno, J.A. Odriozola, Selective hydrodeoxygenation of levulinic acid to γ-valerolactone over Ru supported on functionalized carbon nanofibers, Sustain. Energy Fuels 7 (2023) 857–867, https://doi.org/10.1039/D2SE01503J.
[106] L. Deng, Y. Zhao, J. Li, Y. Fu, B. Liao, Q.-X. Guo, L. Deng, Y. Zhao, J. Li, Y. Fu, Q. Guo, B. Liao, Conversion of levulinic acid and formic acid into γ-valerolactone over heterogeneous catalysts, ChemSusChem 3 (2010) 1172–1175, https://doi.org/10.1002/CSSC.201000163.
[107] C. Michel, J. Zaffran, A.M. Ruppert, J. Matras-Michalska, M. Jędrzejczyk, J. Grams, P. Sautet, Role of water in metal catalyst performance for ketone hydrogenation: a joint experimental and theoretical study on levulinic acid conversion into gamma-valerolactone, Chem. Commun. 50 (2014) 12450–12453, https://doi.org/10.1039/C4CC04401K.
[108] J. Feng, X. Gu, Y. Xue, Y. Han, X. Lu, Production of γ-valerolactone from levulinic acid over a Ru/C catalyst using formic acid as the sole hydrogen source, Sci. Total Environ. 633 (2018) 426–432, https://doi.org/10.1016/J.SCITOTENV.2018.03.209.
[109] C. Fellay, P.J. Dyson, G. Laurenczy, A viable hydrogen-storage system based on selective formic acid decomposition with a ruthenium catalyst, Angew. Chem. 120 (2008) 4030–4032, https://doi.org/10.1002/ANGE.200800320.
[110] D. Sun, A. Ohkubo, K. Asami, T. Katori, Y. Yamada, S. Sato, Vapor-phase hydrogenation of levulinic acid and methyl levulinate to γ-valerolactone over non-noble metal-based catalysts, Mol. Catal. 437 (2017) 105–113, https://doi.org/10.1016/J.MCAT.2017.05.009.
[111] Y. Gao, H. Zhang, A. Han, J. Wang, H.R. Tan, E.S. Tok, S. Jaenicke, G.K. Chuah, Ru/ZrO2 catalysts for transfer hydrogenation of levulinic acid with formic acid/formate mixtures: importance of support stability, ChemistrySelect 3 (2018) 1343–1351, https://doi.org/10.1002/SLCT.201702152.
[112] J. Wang, S. Jaenicke, G.K. Chuah, Zirconium–Beta zeolite as a robust catalyst for the transformation of levulinic acid to γ-valerolactone via Meerwein–Ponndorf–Verley reduction, RSC Adv. 4 (2014) 13481–13489, https://doi.org/10.1039/C4RA01120A.
[113] J.C. Serrano-Ruiz, D.J. Braden, R.M. West, J.A. Dumesic, Conversion of cellulose to hydrocarbon fuels by progressive removal of oxygen, Appl. Catal., B 100 (2010) 184–189, https://doi.org/10.1016/J.APCATB.2010.07.029.
[114] P.A. Son, S. Nishimura, K. Ebitani, Production of γ-valerolactone from biomass-derived compounds using formic acid as a hydrogen source over supported metal catalysts in water solvent, RSC Adv. 4 (2014) 10525–10530, https://doi.org/10.1039/C3RA47580H.
[115] V. Fábos, L.T. Mika, I.T. Horváth, Selective conversion of levulinic and formic acids to γ-valerolactone with the shvo catalyst, Organometallics 33 (2014) 181–187, https://doi.org/10.1021/OM400938H/ASSET/IMAGES/LARGE/OM-2013-00938H_0007. JPEG.
[116] C. Ortiz-Cervantes, J.J. García, Hydrogenation of levulinic acid to γ-valerolactone using ruthenium nanoparticles, Inorg. Chim. Acta. 397 (2013) 124–128, https://doi.org/10.1016/J.ICA.2012.11.031.
[117] G. Amenuvor, B.C.E. Makhubela, J. Darkwa, Efficient solvent-free hydrogenation of levulinic acid to γ-valerolactone by pyrazolylphosphite and pyrazolylphosphinite ruthenium(II) complexes, ACS Sustain. Chem. Eng. 4 (2016) 6010–6018, https://doi.org/10.1021/ACSSUSCHEMENG.6B01281/SUPPL_FILE/SC6B01281_SI_001.PDF.
[118] C. Ortiz-Cervantes, M. Flores-Alamo, J.J. García, Hydrogenation of biomass-derived levulinic acid into γ-valerolactone catalyzed by palladium complexes, ACS Catal. 5 (2015) 1424–1431, https://doi.org/10.1021/CS5020095/SUPPL_FILE/CS5020095_SI_002.CIF.
[119] S.M. Lu, Z. Wang, J. Li, J. Xiao, C. Li, Base-free hydrogenation of CO2 to formic acid in water with an iridium complex bearing a N,N′-diimine ligand, Green Chem. 18 (2016) 4553–4558, https://doi.org/10.1039/C6GC00856A.
[120] N.K. Oklu, B.C.E. Makhubela, Highly selective and efficient solvent-free transformation of bio-derived levulinic acid to γ-valerolactone by Ru(II) arene catalyst precursors, Inorg. Chim. Acta. 482 (2018) 460–468, https://doi.org/10.1016/J.ICA.2018.06.050.
[121] É.A. Enyedy, G.M. Bognár, T. Kiss, M. Hanif, C.G. Hartinger, Solution equilibrium studies on anticancer ruthenium(II)–η6-p-cymene complexes of 3-hydroxy-2(1H)-

pyridones, J. Organomet. Chem. 734 (2013) 38–44, https://doi.org/10.1016/J.JORGANCHEM.2012.10.042.
[122] D.M. Ngumbu, T.A. Kapfunde, N.K. Oklu, B.C.E. Makhubela, Transformation of bio-derived levulinic acid to gamma-valerolactone by cyclopentadienone ruthenium(0) catalyst precursors bearing simple supporting ligands, Appl. Organomet. Chem. 35 (2021) e6243, https://doi.org/10.1002/AOC.6243.
[123] V.S. Shende, A.B. Raut, P. Raghav, A.A. Kelkar, B.M. Bhanage, Room-temperature asymmetric transfer hydrogenation of biomass-derived levulinic acid to optically pure γ-valerolactone using a ruthenium catalyst, ACS Omega 4 (2019) 19491–19498, https://doi.org/10.1021/ACSOMEGA.9B03424/SUPPL_FILE/AO9B03424_SI_001.PDF.
[124] X.L. Du, L. He, S. Zhao, Y.M. Liu, Y. Cao, H.Y. He, K.N. Fan, Hydrogen-independent reductive transformation of carbohydrate biomass into γ-valerolactone and pyrrolidone derivatives with supported gold catalysts, Angew. Chem. Int. Ed. 50 (2011) 7815–7819, https://doi.org/10.1002/ANIE.201100102.
[125] X. Li, J. Li, X. Liu, Q. Tian, C. Hu, The promoting effect of Ce on the performance of Au/CexZr1−xO2 for γ-valerolactone production from biomass-based levulinic acid and formic acid, Catalysts 8 (2018) 241, https://doi.org/10.3390/CATAL8060241, 8 (2018) 241.
[126] P.J. Deuss, K. Barta, J.G. De Vries, Homogeneous catalysis for the conversion of biomass and biomass-derived platform chemicals, Catal. Sci. Technol. 4 (2014) 1174–1196, https://doi.org/10.1039/C3CY01058A.
[127] N. Wang, W. Chu, T. Zhang, X.S. Zhao, Manganese promoting effects on the Co–Ce–Zr–Ox nano catalysts for methane dry reforming with carbon dioxide to hydrogen and carbon monoxide, Chem. Eng. J. 170 (2011) 457–463, https://doi.org/10.1016/J.CEJ.2010.12.042.
[128] P.A. Son, D.H. Hoang, K.T. Canh, The role of gold nanoparticles on different supports for the in-air conversion of levulinic acid into γ-valerolactone with formic acid as an alternative hydrogen source, Russ. J. Appl. Chem. 92 (2019) 1316–1323, https://doi.org/10.1134/S1070427219090179/METRICS.
[129] M. Al-Naji, M. Popova, Z. Chen, N. Wilde, R. Gläser, Aqueous-phase hydrogenation of levulinic acid using formic acid as a sustainable reducing agent over Pt catalysts supported on mesoporous zirconia, ACS Sustain. Chem. Eng. 8 (2020) 393–402, https://doi.org/10.1021/ACSSUSCHEMENG.9B05546/SUPPL_FILE/SC9B05546_SI_001.PDF.
[130] J.K. Padia, C.F.J. Barnard, T.J. Colacot, Dichloro[1,2-bis(diphenylphosphino) ethane]palladium(II), in: Encyclopedia of Reagents for Organic Synthesis, 2009, https://doi.org/10.1002/047084289X.RD097.PUB2.
[131] M. Varkolu, V. Velpula, D.R. Burri, S.R.R. Kamaraju, Gas phase hydrogenation of levulinic acid to γ-valerolactone over supported Ni catalysts with formic acid as hydrogen source, New J. Chem. 40 (2016) 3261–3267, https://doi.org/10.1039/C5NJ02655E.
[132] V. Mohan, C.V. Pramod, M. Suresh, K.H. Prasad Reddy, B.D. Raju, K.S. Rama Rao, Advantage of Ni/SBA-15 catalyst over Ni/MgO catalyst in terms of catalyst stability due to release of water during nitrobenzene hydrogenation to aniline, Catal. Commun. 18 (2012) 89–92, https://doi.org/10.1016/J.CATCOM.2011.11.030.
[133] M. Varkolu, D. Raju Burri, S.R. Rao Kamaraju, S.B. Jonnalagadda, W.E. van Zyl, Hydrogenation of levulinic acid using formic acid as a hydrogen source over Ni/SiO2 catalysts, Chem. Eng. Technol. 40 (2017) 719–726, https://doi.org/10.1002/CEAT.201600429.
[134] S. Gundekari, K. Srinivasan, Screening of solvents, hydrogen source, and investigation of reaction mechanism for the hydrocyclisation of levulinic acid to γ-valerolactone using Ni/SiO2–Al2O3 catalyst, Catal. Lett. 149 (2019) 215–227, https://doi.org/10.1007/S10562-018-2618-7/FIGURES/12.
[135] H. Guo, Y. Hiraga, X. Qi, R.L. Smith, Hydrogen gas-free processes for single-step preparation of transition-metal bifunctional catalysts and one-pot γ-valerolactone synthesis in supercritical CO2-ionic liquid systems, J. Supercrit. Fluids 147 (2019) 263–270, https://doi.org/10.1016/J.SUPFLU.2018.11.010.
[136] A.M. Hengne, A.V. Malawadkar, N.S. Biradar, C.V. Rode, Surface synergism of an Ag–Ni/ZrO2 nanocomposite for the catalytic transfer hydrogenation of bio-derived platform molecules, RSC Adv. 4 (2014) 9730–9736, https://doi.org/10.1039/C3RA46495D.
[137] L.C. Wang, Q. Liu, M. Chen, Y.M. Liu, Y. Cao, H.Y. He, K.N. Fan, Structural evolution and catalytic properties of nanostructured Cu/ZrO2 catalysts prepared by oxalate gel-coprecipitation technique, J. Phys. Chem. C 111 (2007) 16549–16557, https://doi.org/10.1021/JP075930K.
[138] S. Lomate, A. Sultana, T. Fujitani, Effect of SiO2 support properties on the performance of Cu–SiO2 catalysts for the hydrogenation of levulinic acid to gamma valerolactone using formic acid as a hydrogen source, Catal. Sci. Technol. 7 (2017) 3073–3083, https://doi.org/10.1039/C7CY00902J.
[139] V. Mohan, C. Raghavendra, C.V. Pramod, B.D. Raju, K.S. Rama Rao, Ni/H-ZSM-5 as a promising catalyst for vapour phase hydrogenation of levulinic acid at atmospheric pressure, RSC Adv. 4 (2014) 9660–9668, https://doi.org/10.1039/C3RA46485G.
[140] S. Lomate, A. Sultana, T. Fujitani, Vapor phase catalytic transfer hydrogenation (CTH) of levulinic acid to γ-valerolactone over copper supported catalysts using formic acid as hydrogen source, Catal. Lett. 148 (2018) 348–358, https://doi.org/10.1007/S10562-017-2241-Z/FIGURES/10.
[141] M. Ashokraju, V. Mohan, K. Murali, M.V. Rao, B.D. Raju, K.S.R. Rao, Formic acid assisted hydrogenation of levulinic acid to γ -valerolactone over ordered mesoporous Cu/Fe 2O 3 catalyst prepared by hard template method, J. Chem. Sci. 130 (2018) 1–8, https://doi.org/10.1007/S12039-018-1418-3/TABLES/3.
[142] K. Yan, J. Liao, X. Wu, X. Xie, A noble-metal free Cu-catalyst derived from hydrotalcite for highly efficient hydrogenation of biomass-derived furfural and levulinic acid, RSC Adv. 3 (2013) 3853–3856, https://doi.org/10.1039/C3RA22158J.
[143] J.Y. Park, M.A. Kim, S.J. Lee, J. Jung, H.M. Jang, P.P. Upare, Y.K. Hwang, J. S. Chang, J.K. Park, Preparation and characterization of carbon-encapsulated iron nanoparticles and their catalytic activity in the hydrogenation of levulinic acid, J. Mater. Sci. 50 (2015) 334–343, https://doi.org/10.1007/S10853-014-8592-6/FIGURES/8.
[144] K. Yan, A. Chen, Selective hydrogenation of furfural and levulinic acid to biofuels on the ecofriendly Cu–Fe catalyst, Fuel 115 (2014) 101–108, https://doi.org/10.1016/J.FUEL.2013.06.042.
[145] A. Yepez, S. De, M.S. Climent, A.A. Romero, R. Luque, Microwave-assisted conversion of levulinic acid to γ-valerolactone using low-loaded supported iron oxide nanoparticles on porous silicates, Appl. Sci. 5 (2015) 532–543, https://doi.org/10.3390/APP5030532, 5 (2015) 532–543.
[146] S.A. Halawy, S.S. Al-Shihry, M.A. Mohamed, Gas-phase decomposition of formic acid over α-Fe2O3 catalysts, Catal. Lett. 48 (1997) 247–251, https://doi.org/10.1023/A:1019083222147/METRICS.
[147] R.R. Gowda, E.Y.X. Chen, Recyclable earth-abundant metal nanoparticle catalysts for selective transfer hydrogenation of levulinic acid to produce γ-valerolactone, ChemSusChem 9 (2016) 181–185, https://doi.org/10.1002/CSSC.201501402.
[148] J. Wang, G. Zhang, M. Liu, Q. Xia, X. Yu, W. Zhang, J. Shen, C. Yang, X. Jin, Lattice distorted MnCo oxide materials as efficient catalysts for transfer hydrogenation of levulinic acid using formic acid as H-donor, Chem. Eng. Sci. 222 (2020), 115721, https://doi.org/10.1016/J.CES.2020.115721.
[149] K. Kim, J. Kim, Y. Yoon, D. Shin, Effect of the valence states of titanium on the lattice structure and ionic conductivity of Li0.33La0.55TiO3 solid electrolyte, Met. Mater. Int. 20 (2014) 189–194, https://doi.org/10.1007/S12540-013-6033-8/METRICS.
[150] Y. Jiao, W. Hong, P. Li, L. Wang, G. Chen, Metal-organic framework derived Ni/NiO micro-particles with subtle lattice distortions for high-performance electrocatalyst and supercapacitor, Appl. Catal., B 244 (2019) 732–739, https://doi.org/10.1016/J.APCATB.2018.11.035.
[151] Y. Pang, Y. Liu, X. Zhang, M. Gao, H. Pan, Role of particle size, grain size, microstrain and lattice distortion in improved dehydrogenation properties of the ball-milled Mg(AlH4)2, Int. J. Hydrogen Energy 38 (2013) 1460–1468, https://doi.org/10.1016/J.IJHYDENE.2012.11.006.
[152] Y. Liu, X. Hua, C. Xiao, T. Zhou, P. Huang, Z. Guo, B. Pan, Y. Xie, Heterogeneous spin states in ultrathin nanosheets induce subtle lattice distortion to trigger efficient hydrogen evolution, J. Am. Chem. Soc. 138 (2016) 5087–5092, https://doi.org/10.1021/JACS.6B00858/SUPPL_FILE/JA6B00858_SI_001.PDF.
[153] W. Liu, B. Chen, X. Duan, K.H. Wu, W. Qi, X. Guo, B. Zhang, D. Su, Molybdenum carbide modified nanocarbon catalysts for alkane dehydrogenation reactions, ACS Catal. 7 (2017) 5820–5827, https://doi.org/10.1021/ACSCATAL.7B01905/ASSET/IMAGES/LARGE/CS-2017-019055_0008. JPEG.
[154] H. Jin, J. Xie, C. Pan, Z. Zhu, Y. Cheng, C. Zhu, Rhenium-catalyzed acceptorless dehydrogenative coupling via dual activation of alcohols and carbonyl compounds, ACS Catal. 3 (2013) 2195–2198, https://doi.org/10.1021/CS400572Q/SUPPL_FILE/CS400572Q_SI_001.PDF.
[155] O. Mohan, Q.T. Trinh, A. Banerjee, S.H. Mushrif, Predicting CO2 Adsorption and Reactivity on Transition Metal Surfaces Using Popular Density Functional Theory Methods, 2019, pp. 1163–1172, https://doi.org/10.1080/08927022.2019.1632448. Https://Doi.Org/10.1080/08927022.2019.1632448.45.
[156] D.J. Braden, C.A. Henao, J. Heltzel, C.C. Maravelias, J.A. Dumesic, Production of liquid hydrocarbon fuels by catalytic conversion of biomass-derived levulinic acid, Green Chem. 13 (2011) 1755–1765, https://doi.org/10.1039/C1GC15047B.
[157] A. Serrà, R. Artal, L. Philippe, E. Gómez, Electrodeposited Ni-rich Ni-Pt mesoporous nanowires for selective and efficient formic acid-assisted hydrogenation of levulinic acid to γ-valerolactone, Langmuir 37 (2021) 4666–4677, https://doi.org/10.1021/ACS.LANGMUIR.1C00461/ASSET/IMAGES/LARGE/LA1C00461_0007. JPEG.
[158] C. Zhou, Y. Xiao, S. Xu, J. Li, C. Hu, γ-Valerolactone production from furfural residue with formic acid as the sole hydrogen resource via an integrated strategy on Au-Ni/ZrO2, Ind. Eng. Chem. Res. 59 (2020) 17228–17238, https://doi.org/10.1021/ACS.IECR.0C01058/ASSET/IMAGES/LARGE/IE0C01058_0008. JPEG.
[159] E. Soszka, H.M. Reijneveld, M. Jędrzejczyk, I. Rzeźnicka, J. Grams, A.M. Ruppert, Chlorine influence on palladium doped nickel catalysts in levulinic acid hydrogenation with formic acid as hydrogen source, ACS Sustain. Chem. Eng. 6 (2018) 14607–14613, https://doi.org/10.1021/ACSSUSCHEMENG.8B03211/ASSET/IMAGES/LARGE/SC-2018-032114_0002. JPEG.
[160] P.P. Upare, M.G. Jeong, Y.K. Hwang, D.H. Kim, Y.D. Kim, D.W. Hwang, U.H. Lee, J.S. Chang, Nickel-promoted copper–silica nanocomposite catalysts for hydrogenation of levulinic acid to lactones using formic acid as a hydrogen feeder, Appl. Catal. Gen. 491 (2015) 127–135, https://doi.org/10.1016/J.APCATA.2014.12.007.
[161] B. Siyo, M. Schneider, J. Radnik, M.M. Pohl, P. Langer, N. Steinfeldt, Influence of support on the aerobic oxidation of HMF into FDCA over preformed Pd nanoparticle based materials, Appl. Catal. Gen. 478 (2014) 107–116, https://doi.org/10.1016/J.APCATA.2014.03.020.
[162] F. Paquin, J. Rivnay, A. Salleo, N. Stingelin, C. Silva-Acuña, Multi-phase microstructures drive exciton dissociation in neat semicrystalline polymeric semiconductors, J Mater Chem C Mater 3 (2015) 10715–10722, https://doi.org/10.1039/C5TC02043C.
[163] Y. Román-Leshkov, C.J. Barrett, Z.Y. Liu, J.A. Dumesic, Production of dimethylfuran for liquid fuels from biomass-derived carbohydrates, Nature 447 (2007) 7147, https://doi.org/10.1038/nature05923, 447 (2007) 982–985.

[164] H. Cai, C. Li, A. Wang, T. Zhang, Biomass into chemicals: one-pot production of furan-based diols from carbohydrates via tandem reactions, Catal. Today 234 (2014) 59–65, https://doi.org/10.1016/J.CATTOD.2014.02.029.
[165] R. Alamillo, M. Tucker, M. Chia, Y. Pagán-Torres, J. Dumesic, The selective hydrogenation of biomass-derived 5-hydroxymethylfurfural using heterogeneous catalysts, Green Chem. 14 (2012) 1413–1419, https://doi.org/10.1039/C2GC35039D.
[166] G. Wang, Z. Zhang, L. Song, Efficient and selective alcoholysis of furfuryl alcohol to alkyl levulinates catalyzed by double SO 3 H-functionalized ionic liquids, Green Chem. 16 (2014) 1436–1443, https://doi.org/10.1039/C3GC41693C.
[167] M. Braun, M. Antonietti, A continuous flow process for the production of 2,5-dimethylfuran from fructose using (non-noble metal based) heterogeneous catalysis, Green Chem. 19 (2017) 3813–3819, https://doi.org/10.1039/C7GC01055A.
[168] C.C. Chang, S.K. Green, C.L. Williams, P.J. Dauenhauer, W. Fan, Ultra-selective cycloaddition of dimethylfuran for renewable p-xylene with H-BEA, Green Chem. 16 (2014) 585–588, https://doi.org/10.1039/C3GC40740C.
[169] D.A. Rothamer, J.H. Jennings, Study of the knocking propensity of 2,5-dimethylfuran–gasoline and ethanol–gasoline blends, Fuel 98 (2012) 203–212, https://doi.org/10.1016/J.FUEL.2012.03.049.
[170] Q. Zhang, G. Chen, Z. Zheng, H. Liu, J. Xu, M. Yao, Combustion and emissions of 2,5-dimethylfuran addition on a diesel engine with low temperature combustion, Fuel 103 (2013) 730–735, https://doi.org/10.1016/J.FUEL.2012.08.045.
[171] R. Daniel, G. Tian, H. Xu, M.L. Wyszynski, X. Wu, Z. Huang, Effect of spark timing and load on a DISI engine fuelled with 2,5-dimethylfuran, Fuel 90 (2011) 449–458, https://doi.org/10.1016/J.FUEL.2010.10.008.
[172] J. Mitra, X. Zhou, T. Rauchfuss, Pd/C-catalyzed reactions of HMF: decarbonylation, hydrogenation, and hydrogenolysis, Green Chem. 17 (2014) 307–313, https://doi.org/10.1039/C4GC01520G.
[173] T. Wang, J. Zhang, W. Xie, Y. Tang, D. Guo, Y. Ni, Catalytic transfer hydrogenation of biobased HMF to 2,5-bis-(Hydroxymethyl)Furan over Ru/Co3O4, Catalysts 7 (2017) 92, https://doi.org/10.3390/CATAL7030092, 97 (2017) 92.
[174] J.M. Timko, D.J. Cram, The furanyl unit in host compounds, J. Am. Chem. Soc. 96 (1974) 7159–7160, https://doi.org/10.1021/JA00829A085/ASSET/JA00829A085.FP.PNG_V03.
[175] C. Zeng, H. Seino, J. Ren, K. Hatanaka, N. Yoshie, Self-healing bio-based furan polymers cross-linked with various bis-maleimides, Polymer (Guildf) 54 (2013) 5351–5357, https://doi.org/10.1016/J.POLYMER.2013.07.059.
[176] T. Thananatthanachon, T.B. Rauchfuss, Efficient production of the liquid fuel 2,5-dimethylfuran from fructose using formic acid as a reagent, Angew. Chem. 122 (2010) 6766–6768, https://doi.org/10.1002/ANGE.201002267.
[177] B. Hu, L. Warczinski, X. Li, M. Lu, J. Bitzer, M. Heidelmann, T. Eckhard, Q. Fu, J. Schulwitz, M. Merko, M. Li, W. Kleist, C. Hättig, M. Muhler, B. Peng, Formic acid-assisted selective hydrogenolysis of 5-hydroxymethylfurfural to 2,5-dimethylfuran over bifunctional Pd nanoparticles supported on N-doped mesoporous carbon, Angew. Chem. Int. Ed. 60 (2021) 6807–6815, https://doi.org/10.1002/ANIE.202012816.
[178] P. Wu, D. Zhao, G. Lu, C. Cai, Supported Pd–Au bimetallic nanoparticles as an efficient catalyst for the hydrodeoxygenation of vanillin with formic acid at room temperature, Green Chem. 24 (2022) 1096–1102, https://doi.org/10.1039/D1GC04240H.
[179] L. Tao, T.H. Yan, W. Li, Y. Zhao, Q. Zhang, Y.M. Liu, M.M. Wright, Z.H. Li, H. Y. He, Y. Cao, Toward an integrated conversion of 5-hydroxymethylfurfural and ethylene for the production of renewable p-xylene, Chem 4 (2018) 2212–2227, https://doi.org/10.1016/J.CHEMPR.2018.07.007.
[180] J. Zhao, M. Liu, G. Fan, L. Yang, F. Li, Efficient transfer hydrogenolysis of 5-hydromethylfurfural to 2,5-dimethylfuran over CoFe bimetallic catalysts using formic acid as a sustainable hydrogen donor, Ind. Eng. Chem. Res. 60 (2021) 5826–5837, https://doi.org/10.1021/ACS.IECR.1C01029/ASSET/IMAGES/LARGE/IE1C01029_0015. JPEG.
[181] P. Yang, Q. Xia, X. Liu, Y. Wang, Catalytic transfer hydrogenation/hydrogenolysis of 5-hydroxymethylfurfural to 2,5-dimethylfuran over Ni-Co/C catalyst, Fuel 187 (2017) 159–166, https://doi.org/10.1016/J.FUEL.2016.09.026.
[182] Z. Fu, Z. Wang, W. Lin, W. Song, Conversion of Furan Derivatives for Preparation of Biofuels over Ni–Cu/C Catalyst, vol. 39, 2017, pp. 1176–1181, https://doi.org/10.1080/15567036.2017.1310959. Http://Dx.Doi.Org/10.1080/15567036.2017.1310959.
[183] T. Thananatthanachon, T.B. Rauchfuss, Efficient route to hydroxymethylfurans from sugars via transfer hydrogenation, ChemSusChem 3 (2010) 1139–1141, https://doi.org/10.1002/CSSC.201000209.
[184] V. Parmon, G. Centi, M. Al-Dahhan, D. Aranda, F. Fajula, F. Frusteri, H. Garcia, E. Heeres, E. Hensen, W. Leitner, International Scientific Committee, (n.d.).
[185] S. Goswami, S. Dey, S. Jana, Design and synthesis of a unique ditopic macrocyclic fluorescent receptor containing furan ring as a spacer for the recognition of dicarboxylic acids, Tetrahedron 64 (2008) 6358–6363, https://doi.org/10.1016/J.TET.2008.04.086.
[186] L. Xu, R. Nie, X. Chen, Y. Li, Y. Jiang, X. Lu, Formic acid enabled selectivity boosting in transfer hydrogenation of 5-hydroxymethylfurfural to 2,5-furandimethanol on highly dispersed Co–Nx sites, Catal. Sci. Technol. 11 (2021) 1451–1457, https://doi.org/10.1039/D0CY01969K.
[187] J. Tuteja, H. Choudhary, S. Nishimura, K. Ebitani, Direct synthesis of 1,6-hexanediol from HMF over a heterogeneous Pd/ZrP catalyst using formic acid as hydrogen source, ChemSusChem 7 (2014) 96–100, https://doi.org/10.1002/CSSC.201300832.
[188] C. Xiong, Y. Sun, J. Du, W. Chen, Z. Si, H. Gao, X. Tang, X. Zeng, Efficient conversion of fructose to 5-[(formyloxy)methyl]furfural by reactive extraction and in-situ esterification, Kor. J. Chem. Eng. 35 (2018) 1312–1318, https://doi.org/10.1007/S11814-018-0025-9/METRICS.
[189] Y. Jiang, W. Chen, Y. Sun, Z. Li, X. Tang, X. Zeng, L. Lin, S. Liu, One-pot conversion of biomass-derived carbohydrates into 5-[(formyloxy)methyl]furfural: a novel alternative platform chemical, Ind. Prod. 83 (2016) 408–413, https://doi.org/10.1016/J.INDCROP.2016.01.004.
[190] Y. Sun, C. Xiong, Q. Liu, J. Zhang, X. Tang, X. Zeng, S. Liu, L. Lin, Catalytic transfer hydrogenolysis/hydrogenation of biomass-derived 5-formyloxymethylfurfural to 2, 5-dimethylfuran over Ni-Cu bimetallic catalyst with formic acid as a hydrogen donor, Ind. Eng. Chem. Res. 58 (2019) 5414–5422, https://doi.org/10.1021/ACS.IECR.8B05960/ASSET/IMAGES/LARGE/IE-2018-05960V_0009. JPEG.
[191] J.J. Bozell, L. Moens, D.C. Elliott, Y. Wang, G.G. Neuenscwander, S.W. Fitzpatrick, R.J. Bilski, J.L. Jarnefeld, Production of levulinic acid and use as a platform chemical for derived products, Resour. Conserv. Recycl. 28 (2000) 227–239, https://doi.org/10.1016/S0921-3449(99)00047-6.
[192] J.J. Bozell, G.R. Petersen, Technology development for the production of biobased products from biorefinery carbohydrates—the US Department of Energy's "Top 10" revisited, Green Chem. 12 (2010) 539–554, https://doi.org/10.1039/B922014C.
[193] K. Yan, G. Wu, T. Lafleur, C. Jarvis, Production, properties and catalytic hydrogenation of furfural to fuel additives and value-added chemicals, Renew. Sustain. Energy Rev. 38 (2014) 663–676, https://doi.org/10.1016/J.RSER.2014.07.003.
[194] Y. Nakagawa, M. Tamura, K. Tomishige, Catalytic reduction of biomass-derived furanic compounds with hydrogen, ACS Catal. 3 (2013) 2655–2668, https://doi.org/10.1021/CS400616P/ASSET/IMAGES/LARGE/CS-2013-00616P_0037. JPEG.
[195] V.V. Pushkarev, N. Musselwhite, K. An, S. Alayoglu, G.A. Somorjai, High structure sensitivity of vapor-phase furfural decarbonylation/hydrogenation reaction network as a function of size and shape of Pt nanoparticles, Nano Lett. 12 (2012) 5196–5201, https://doi.org/10.1021/NL3023127/SUPPL_FILE/NL3023127_SI_001.PDF.
[196] F.H. Isikgor, C.R. Becer, Lignocellulosic biomass: a sustainable platform for the production of bio-based chemicals and polymers, Polym. Chem. 6 (2015) 4497–4559, https://doi.org/10.1039/C5PY00263J.
[197] Furfuryl Alcohol and Lignin Adhesive Composition, 2002.
[198] J. Li, D.J. Ding, L.J. Xu, Q.X. Guo, Y. Fu, The breakdown of reticent biomass to soluble components and their conversion to levulinic acid as a fuel precursor, RSC Adv. 4 (2014) 14985–14992, https://doi.org/10.1039/C3RA47923D.
[199] C.K.P. Neeli, Y.M. Chung, W.S. Ahn, Catalytic transfer hydrogenation of furfural to furfuryl alcohol by using ultrasmall Rh nanoparticles embedded on diamine-functionalized KIT-6, ChemCatChem 9 (2017) 4570–4579, https://doi.org/10.1002/CCTC.201701037.
[200] P. Nagaiah, P. Gidyonu, M. Ashokraju, M.V. Rao, P. Challa, D.R. Burri, S.R. R. Kamaraju, Magnesium aluminate supported Cu catalyst for selective transfer hydrogenation of biomass derived furfural to furfuryl alcohol with formic acid as hydrogen donor, ChemistrySelect 4 (2019) 145–151, https://doi.org/10.1002/SLCT.201803645.
[201] J. Du, J. Zhang, Y. Sun, W. Jia, Z. Si, H. Gao, X. Tang, X. Zeng, T. Lei, S. Liu, L. Lin, Catalytic transfer hydrogenation of biomass-derived furfural to furfuryl alcohol over in-situ prepared nano Cu-Pd/C catalyst using formic acid as hydrogen source, J. Catal. 368 (2018) 69–78, https://doi.org/10.1016/J.JCAT.2018.09.025.
[202] M. Ojeda, E. Iglesia, kPa Hcooh, at kPa HCOOH, M. Ojeda, E. Iglesia, Formic acid dehydrogenation on Au-based catalysts at near-ambient temperatures, Angew. Chem. 121 (2009) 4894–4897, https://doi.org/10.1002/ANGE.200805723.
[203] S. Sitthisa, D.E. Resasco, Hydrodeoxygenation of furfural over supported metal catalysts: a comparative study of Cu, Pd and Ni, Catal. Lett. 141 (2011) 784–791, https://doi.org/10.1007/S10562-011-0581-7/FIGURES/5.
[204] J. Kijeński, P. Winiarek, T. Paryjczak, A. Lewicki, A. Mikolajska, Platinum deposited on monolayer supports in selective hydrogenation of furfural to furfuryl alcohol, Appl. Catal. Gen. 233 (2002) 171–182, https://doi.org/10.1016/S0926-860X(02)00140-0.
[205] L. Xu, R. Nie, X. Lyu, J. Wang, X. Lu, Selective hydrogenation of furfural to furfuryl alcohol without external hydrogen over N-doped carbon confined Co catalysts, Fuel Process. Technol. 197 (2020), 106205, https://doi.org/10.1016/J.FUPROC.2019.106205.
[206] A. Bohre, S. Dutta, B. Saha, M.M. Abu-Omar, Upgrading furfurals to drop-in biofuels: an overview, ACS Sustain. Chem. Eng. 3 (2015) 1263–1277, https://doi.org/10.1021/ACSSUSCHEMENG.5B00271/ASSET/IMAGES/LARGE/SC-2015-00271A_0014. JPEG.
[207] Z. Fu, Z. Wang, W. Lin, W. Song, S. Li, High efficient conversion of furfural to 2-methylfuran over Ni-Cu/Al2O3 catalyst with formic acid as a hydrogen donor, Appl. Catal. Gen. 547 (2017) 248–255, https://doi.org/10.1016/J.APCATA.2017.09.011.
[208] K. Razmgar, M. Altarawneh, I. Oluwoye, G. Senanayake, Selective hydrogenation of 1,3-butadiene over ceria catalyst: a molecular insight, Mol. Catal. 524 (2022), 112331, https://doi.org/10.1016/J.MCAT.2022.112331.
[209] Q.C. Wei, Y. Chen, Z. Wang, D.Z. Yu, W.H. Wang, J.Q. Li, L.H. Chen, Y. Li, B.L. Su, Light-assisted semi-hydrogenation of 1,3-butadiene with water, Angew. Chem. Int. Ed. 61 (2022), e202210573, https://doi.org/10.1002/ANIE.202210573.
[210] D.H. Carrales-Alvarado, A.B. Dongil, A. Guerrero-Ruiz, I. Rodríguez-Ramos, Tandem catalysts for the selective hydrogenation of butadiene with hydrogen

generated from the decomposition of formic acid, Chem. Commun. 57 (2021) 6479–6482, https://doi.org/10.1039/D1CC01954F.
[211] V.L. Yfanti, A.A. Lemonidou, Effect of hydrogen donor on glycerol hydrodeoxygenation to 1,2-propanediol, Catal. Today 355 (2020) 727–736, https://doi.org/10.1016/J.CATTOD.2019.04.080.
[212] I. Gandarias, P.L. Arias, S.G. Fernández, J. Requies, M. el Doukkali, M.B. Güemez, Hydrogenolysis through catalytic transfer hydrogenation: glycerol conversion to 1,2-propanediol, Catal. Today 195 (2012) 22–31, https://doi.org/10.1016/J.CATTOD.2012.03.067.
[213] I. Gandarias, J. Requies, P.L. Arias, U. Armbruster, A. Martin, Liquid-phase glycerol hydrogenolysis by formic acid over Ni–Cu/Al2O3 catalysts, J. Catal. 290 (2012) 79–89, https://doi.org/10.1016/J.JCAT.2012.03.004.
[214] J. Yuan, S. Li, L. Yu, Y. Liu, Y. Cao, Efficient catalytic hydrogenolysis of glycerol using formic acid as hydrogen source, Chin. J. Catal. 34 (2013) 2066–2074, https://doi.org/10.1016/S1872-2067(12)60656-1.
[215] P. Makowski, R. Demir Cakan, M. Antonietti, F. Goettmann, M.M. Titirici, Selective partial hydrogenation of hydroxy aromatic derivatives with palladium nanoparticles supported on hydrophilic carbon, Chem. Commun. (2008) 999–1001, https://doi.org/10.1039/B717928F, 0.
[216] J. Morales, R. Hutcheson, C. Noradoun, I.F. Cheng, Hydrogenation of phenol by the Pd/Mg and Pd/Fe bimetallic systems under mild reaction conditions, Ind. Eng. Chem. Res. 41 (2002) 3071–3074, https://doi.org/10.1021/IE0200510/ASSET/IMAGES/LARGE/IE0200510F00002. JPEG.
[217] D. Zhang, F. Ye, T. Xue, Y. Guan, Y.M. Wang, Transfer hydrogenation of phenol on supported Pd catalysts using formic acid as an alternative hydrogen source, Catal. Today 234 (2014) 133–138, https://doi.org/10.1016/J.CATTOD.2014.02.039.
[218] P. Sudakar, G.H. Gunasekar, I.H. Baek, S. Yoon, Recyclable and efficient heterogenized Rh and Ir catalysts for the transfer hydrogenation of carbonyl compounds in aqueous medium, Green Chem. 18 (2016) 6456–6461, https://doi.org/10.1039/C6GC02195F.
[219] Y. Gao, S. Jaenicke, G.K. Chuah, Highly efficient transfer hydrogenation of aldehydes and ketones using potassium formate over AlO(OH)-entrapped ruthenium catalysts, Appl. Catal. Gen. 484 (2014) 51–58, https://doi.org/10.1016/J.APCATA.2014.07.010.
[220] Z. Wang, L. Huang, L. Geng, R. Chen, W. Xing, Y. Wang, J. Huang, Chemoselective transfer hydrogenation of aldehydes and ketones with a heterogeneous iridium catalyst in water, Catal. Lett. 145 (2015) 1008–1013, https://doi.org/10.1007/S10562-014-1473-4/TABLES/3.
[221] K. Jacobson, K.C. Maheria, A. Kumar Dalai, Bio-oil valorization: a review, Renew. Sustain. Energy Rev. 23 (2013) 91–106, https://doi.org/10.1016/J.RSER.2013.02.036.
[222] A.K. Mondal, C. Qin, A.J. Ragauskas, Y. Ni, F. Huang, G. Zhuang, Hydrogenation of Pyrolysis Oil from Loblolly Pine Residue, vol. 5, Paper and Biomaterials, 2020, pp. 1–13, https://doi.org/10.12103/J.ISSN.2096-2355.2020.01.001.
[223] M.M. Dell'Anna, V.F. Capodiferro, M. Mali, D. Manno, P. Cotugno, A. Monopoli, P. Mastrorilli, Highly selective hydrogenation of quinolines promoted by recyclable polymer supported palladium nanoparticles under mild conditions in aqueous medium, Appl. Catal. Gen. 481 (2014) 89–95, https://doi.org/10.1016/J.APCATA.2014.04.041.
[224] L. Tao, Q. Zhang, S.S. Li, X. Liu, Y.M. Liu, Y. Cao, Heterogeneous gold-catalyzed selective reductive transformation of quinolines with formic acid, Adv. Synth. Catal. 357 (2015) 753–760, https://doi.org/10.1002/ADSC.201400721.
[225] B. Vilhanová, J.A. van Bokhoven, M. Ranocchiari, Gold particles supported on amino-functionalized silica catalyze transfer hydrogenation of N-heterocyclic compounds, Adv. Synth. Catal. 359 (2017) 677–686, https://doi.org/10.1002/ADSC.201601147.
[226] J.R. Cabrero-Antonino, R. Adam, K. Junge, R. Jackstell, M. Beller, Cobalt-catalysed transfer hydrogenation of quinolines and related heterocycles using formic acid under mild conditions, Catal. Sci. Technol. 7 (2017) 1981–1985, https://doi.org/10.1039/C7CY00437K.
[227] G. Li, H. Yang, H. Zhang, Z. Qi, M. Chen, W. Hu, L. Tian, R. Nie, W. Huang, Encapsulation of nonprecious metal into ordered mesoporous N-doped carbon for efficient quinoline transfer hydrogenation with formic acid, ACS Catal. 8 (2018) 8396–8405, https://doi.org/10.1021/ACSCATAL.8B01404/SUPPL_FILE/CS8B01404_SI_001.PDF.
[228] C.A. Smith, F. Brandi, M. Al-Naji, R. Guterman, Resin-supported iridium complex for low-temperature vanillin hydrogenation using formic acid in water, RSC Adv. 11 (2021) 15835–15840, https://doi.org/10.1039/D1RA01460A.
[229] L. Wang, J. Zhang, G. Wang, W. Zhang, C. Wang, C. Bian, F.S. Xiao, Selective hydrogenolysis of carbon–oxygen bonds with formic acid over a Au–Pt alloy catalyst, Chem. Commun. 53 (2017) 2681–2684, https://doi.org/10.1039/C6CC09599B.
[230] R. Nie, X. Peng, H. Zhang, X. Yu, X. Lu, D. Zhou, Q. Xia, Transfer hydrogenation of bio-fuel with formic acid over biomass-derived N-doped carbon supported acid-resistant Pd catalyst, Catal. Sci. Technol. 7 (2017) 627–634, https://doi.org/10.1039/C6CY02461K.
[231] C. Pu, J. Zhang, G. Chang, Y. Xiao, X. Ma, J. Wu, T. Luo, K. Huang, S. Ke, J. Li, X. Yang, Nitrogen precursor-mediated construction of N-doped hierarchically porous carbon-supported Pd catalysts with controllable morphology and composition, Carbon N Y 159 (2020) 451–460, https://doi.org/10.1016/j.carbon.2019.12.058.
[232] H. Yang, R. Nie, W. Xia, X. Yu, D. Jin, X. Lu, D. Zhou, Q. Xia, Co embedded within biomass-derived mesoporous N-doped carbon as an acid-resistant and chemoselective catalyst for transfer hydrodeoxygenation of biomass with formic acid, Green Chem. 19 (2017) 5714–5722, https://doi.org/10.1039/C7GC02648J.
[233] S. Zhou, F. Dai, C. Dang, M. Wang, D. Liu, F. Lu, H. Qi, Scale-up biopolymer-chelated fabrication of cobalt nanoparticles encapsulated in N-enriched graphene shells for biofuel upgrade with formic acid, Green Chem. 21 (2019) 4732–4747, https://doi.org/10.1039/C9GC01720H.
[234] M. Duan, Q. Cheng, M. Wang, Y. Wang, In situ hydrodeoxygenation of vanillin over Ni–Co–P/HAP with formic acid as a hydrogen source, RSC Adv. 11 (2021) 10996–11003, https://doi.org/10.1039/D1RA00979F.
[235] A. Rahimi, A. Ulbrich, J.J. Coon, S.S. Stahl, Formic-acid-induced depolymerization of oxidized lignin to aromatics, Nature 515 (2014) 7526, https://doi.org/10.1038/nature13867, 515 (2014) 249–252.
[236] J. Park, A. Riaz, D. Verma, H.J. Lee, H.M. Woo, J. Kim, Fractionation of lignocellulosic biomass over core–shell Ni@Al2O3 catalysts with formic acid as a cocatalyst and hydrogen source, ChemSusChem 12 (2019) 1743–1762, https://doi.org/10.1002/CSSC.201802847.
[237] M. Oregui-Bengoechea, I. Gandarias, P.L. Arias, T. Barth, Unraveling the role of formic acid and the type of solvent in the catalytic conversion of lignin: a holistic approach, ChemSusChem 10 (2017) 754–766, https://doi.org/10.1002/CSSC.201601410.
[238] M. Oregui-Bengoechea, I. Gandarias, N. Miletić, S.F. Simonsen, A. Kronstad, P. L. Arias, T. Barth, Thermocatalytic conversion of lignin in an ethanol/formic acid medium with NiMo catalysts: role of the metal and acid sites, Appl. Catal., B 217 (2017) 353–364, https://doi.org/10.1016/J.APCATB.2017.06.004.